

FIG. 5. IL-6 enhances GSIS through the PLC-dependent pathway. **A:** Pancreatic islets isolated from 8-week-old C57BL/6N mice were pretreated with vehicle or 2 $\mu\text{mol/L}$ U-73122 with or without concomitant 1,200 pg/mL IL-6 for 24 h, followed by measurement of insulin secretion for 60 min in KRBB supplemented with either 1.67 or 16.7 mmol/L glucose ($n = 5$ per group). ** $P < 0.01$ vs. insulin secretion from isolated islets without IL-6 pretreatment assessed by one-way ANOVA followed by Bonferroni's post hoc test. **B** and **C:** MIN-6 cells were pretreated with vehicle or a pharmacological inhibitor (2 $\mu\text{mol/L}$ U-73122 [**B**] 1.5 mmol/L neomycin [**C**]) with or without concomitant 1,200 pg/mL IL-6 for 24 h, followed by measurement of insulin secretion for 60 min in KRBB supplemented with either 1.67 or 16.7 mmol/L glucose ($n = 6$ per group). ** $P < 0.01$ vs. insulin secretion from MIN-6 cells without IL-6 pretreatment assessed by one-way ANOVA followed by Bonferroni's post hoc test. **D:** MIN-6 cells were transfected with NT siRNA or the specific siRNA for each PLC isoform for 24 h and then incubated with or without concomitant 1,200 pg/mL recombinant IL-6 for 24 h, followed by examination of insulin secretion for 60 min in KRBB supplemented with 16.7 mmol/L glucose ($n = 5$ per group). ** $P < 0.01$ vs. insulin secretion from MIN-6 cells without IL-6 pretreatment assessed by one-way ANOVA followed by Bonferroni's post hoc test. Data are presented as means \pm SE.

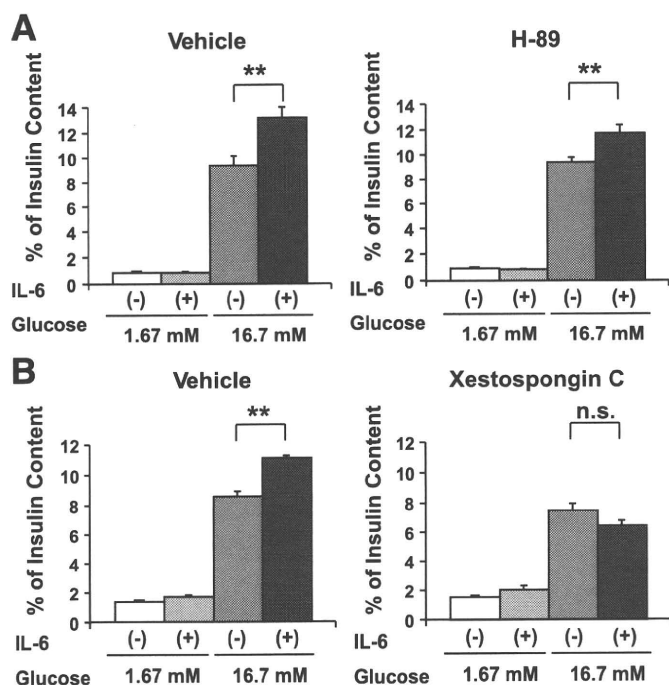


FIG. 6. IL-6-induced enhancement of GSIS is abrogated by an IP₃ receptor antagonist but not by a PKA inhibitor. MIN-6 cells were pretreated with vehicle or a pharmacological inhibitor (1 μmol/L H-89 [A] or 10 μmol/L Xestosponginc C [B]) with or without concomitant 1,200 pg/mL IL-6 for 24 h, followed by measurement of insulin secretion for 60 min in KRBB supplemented with either 1.67 or 16.7 mmol/L glucose ($n = 6$ per group). ** $P < 0.01$ vs. insulin secretion from MIN-6 cells without IL-6 pretreatment assessed by one-way ANOVA followed by Bonferroni's post hoc test. Data are presented as means \pm SE.

consistent effects of IL-6 on insulin secretion have not been reported. At 1,500 pg/mL, IL-6 increased basal insulin secretion from murine isolated islets (4), and at 100 pg/mL, IL-6 increased both basal and glucose-stimulated insulin secretion from HIT-15 cells, a hamster β -cell line (5). On the other hand, 500–2,000 pg/mL (6) or 200–2,000 pg/mL (7) of IL-6 decreased GSIS from rat isolated pancreatic islets and 400 pg/mL IL-6 decreased GSIS from mouse isolated pancreatic islets (8). Furthermore, 400,000 pg/mL IL-6 did not alter insulin secretion from MIN-6 cells (9). Although the reason is unclear, these inconsistencies might be due to the different IL-6 concentrations and preincubation periods as well as sources of pancreatic β -cells used in the experiments. Therefore, in the current study, to elucidate the role of obesity-induced hyper-IL-6emia in insulin secretion, we focused on IL-6 concentrations within the range of those observed in *ob/ob* and *db/db* mice, 150–7,000 pg/mL (20–22) in both in vivo and in vitro experiments. In addition, a circulating IL-6 level as high as 3,400 pg/mL was reported in obese human subjects (41). In the present in vivo study, plasma IL-6 concentrations were elevated and remained at 900–1,400 pg/mL during first the 10 days after adenoviral IL-6 expression in the liver. We used a similar concentration, 1,200 pg/mL, of IL-6 in our in vitro experiments.

We analyzed IL-6 effects on insulin secretion comparing three different settings of pancreatic β -cells, i.e., murine in vivo, isolated pancreatic islets ex vivo, and a pancreatic β -cell line, MIN-6 cells in vitro. Notably, all experiments showed IL-6-induced enhancement of GSIS, suggesting a direct effect of IL-6 on pancreatic β -cells. In addition, IL-6R knockdown, PLC inhibitors, and an IP₃ receptor

antagonist almost completely inhibited the IL-6-induced enhancement of GSIS. PLC activation reportedly leads to hydrolysis of PIP₂ into diacylglycerol and IP₃. IP₃ binds to the IP₃ receptor on the ER, resulting in the induction of Ca²⁺ release from the ER. This raises the cytoplasmic free Ca²⁺ concentration and subsequently enhances insulin secretion (39). Our findings indicate that activation of the PLC-IP₃-dependent pathway by IL-6 appears to play a major role in GSIS enhancement during hyper-IL-6-emia. Activation of the PLC pathway by IL-6 signaling has been reported in several cell types. For instance, direct association of gp130 and PLC- γ was shown in a Ewing's sarcoma cell line (33). Activation of PLC- γ ₁ by IL-6 was also reported in a pheochromocytoma cell line (34). On the other hand, in this study, siRNA experiments revealed knockdown of PLC- β ₁, but not other isoforms, significantly to blunt IL-6-induced GSIS. Because the degrees of expression suppression differed among siRNAs specific for each PLC isoform (Supplementary Fig. 1), these results do not exclude the possibility that other PLC isoforms contribute to IL-6-induced GSIS. However, the data strongly suggest involvement of PLC- β ₁ itself in the underlying mechanism. PLC- β ₁ is reportedly activated by G protein-coupled receptors (42). Taken together with the results that long incubation periods, i.e., 24 h, were required for the stimulatory effects of IL-6 on GSIS, unknown mechanisms involving transcriptional or posttranscriptional alterations in certain molecules might mediate between the IL-6R and G protein-coupled receptor pathways.

Stimulatory effects of IL-6 on GSIS were also suggested in IL-6-KO mice (3). In HF-fed IL-6-KO mice, GSIS was impaired without alterations in pancreatic β -cell mass, resulting in postprandial hyperglycemia. The authors mainly analyzed the effects of IL-6 on pancreatic α -cell expansion, since IL-6-KO mice exhibited low glucagon levels with impaired pancreatic α -cell expansion (3). In the current study, plasma glucagon concentrations were significantly higher in IL-6 mice. In addition, interestingly, IL-6 enhanced GSIS more robustly in vivo and in isolated islets than that in MIN-6 cells (compare Fig. 3B and 4A with 4B). These findings suggest that the effects of IL-6 on glucagon secretion from pancreatic α -cells may have some impact on insulin secretion from β -cells in both in vivo and ex vivo experiments, in addition to the direct effects of IL-6 on β -cells.

Is the observed IL-6-mediated enhancement of GSIS involved in physiological or pathological states? Obesity leads to elevation of circulating IL-6. Circulating IL-6 is reportedly related to fat mass, and this relationship is also observed in mildly obese human subjects (43), suggesting that circulating IL-6 increases in the early phase of obesity. Notably, in human subjects, early in the development of obesity, GSIS is enhanced (44), and insulin hypersecretion occurs before blood glucose elevation (45–47). In mice, IL-6 deficiency reportedly raises postprandial blood glucose levels after HF diet loading (48) mainly due to impaired GSIS (3). In addition, in human subjects, circulating IL-6 concentrations correlate positively with first-phase insulin secretion, and this correlation is independent of insulin resistance (11). Taken together, these observations suggest that the mechanism elucidated in this study might be involved in GSIS enhancement in the early stage of obesity development. We recently identified a neuronal pathway from the liver as being involved in hyperinsulinemia in obese mice (17). In this regard, insulin hypersecretion during obesity development appears to be mediated by both neuronal and humoral signals, which are thought to cooperatively regulate

systemic metabolism (49). These mechanisms likely contribute to maintaining glucose homeostasis during obesity development. Interestingly, during septic shock states, hypoglycemia is commonly observed and this phenomenon is explained by hyperinsulinemia (50,51). It is well-known that IL-6 is markedly elevated during septic shock. Collectively, our findings suggest that hyper-IL-6-emia is involved in the development of hyperinsulinemia in states of both obesity and septic shock.

In conclusion, *in vivo*, *ex vivo*, and *in vitro* experiments consistently demonstrated that IL-6 enhances GSIS from pancreatic β -cells and that this enhancement of GSIS is likely to be mediated by the PLC-IP₃-dependent pathway. Modulating the PLC pathway in pancreatic β -cells is a potential therapeutic strategy for achieving efficient post-prandial insulin secretion.

ACKNOWLEDGMENTS

This work was supported by Grants-in-Aid for Scientific Research to H.K. (B2, 15390282) and Y.O. (A2, 19209034) from the Ministry of Education, Science, Sports and Culture of Japan and a Grant-in-Aid for Scientific Research (H19-genome-005) to Y.O. from the Ministry of Health, Labor and Welfare of Japan. This work was also supported by the Global-COE Program for Network Medicine to Y.O. and H.K. from the Ministry of Education, Culture, Sports, Science and Technology of Japan.

No potential conflicts of interest relevant to this article were reported.

T.S. and J.I. researched data, wrote the article, and contributed to discussion. T.Y., Y.I., K.K., K.U., Y.H., and H.I. contributed to discussion. Y.O. contributed to discussion and reviewed and edited the article. H.K. contributed to discussion and wrote the article.

The authors thank I. Sato, J. Fushimi, M. Aizawa, M. Hoshi, and T. Takasugi (Department of Metabolic Diseases, Center for Metabolic Diseases, Tohoku University Graduate School of Medicine) for technical support.

REFERENCES

- Kristiansen OP, Mandrup-Poulsen T. Interleukin-6 and diabetes: the good, the bad, or the indifferent? *Diabetes* 2005;54(Suppl. 2):S114-S124
- Hoene M, Weigert C. The role of interleukin-6 in insulin resistance, body fat distribution and energy balance. *Obes Rev* 2008;9:20-29
- Ellingsgaard H, Ehlers JA, Hammar EB, et al. Interleukin-6 regulates pancreatic alpha-cell mass expansion. *Proc Natl Acad Sci USA* 2008;105:13163-13168
- Buschard K, Aaen K, Horn T, Van Damme J, Bendtzen K. Interleukin 6: a functional and structural *in vitro* modulator of beta-cells from islets of Langerhans. *Autoimmunity* 1990;5:185-194
- Shimizu H, Ohtani K, Kato Y, Mori M. Interleukin-6 increases insulin secretion and preproinsulin mRNA expression via Ca²⁺-dependent mechanism. *J Endocrinol* 2000;166:121-126
- Sandler S, Bendtzen K, Eizirik DL, Welsh M. Interleukin-6 affects insulin secretion and glucose metabolism of rat pancreatic islets *in vitro*. *Endocrinology* 1990;126:1288-1294
- Southern C, Schulster D, Green IC. Inhibition of insulin secretion from rat islets of Langerhans by interleukin-6. An effect distinct from that of interleukin-1. *Biochem J* 1990;272:243-245
- Handschin C, Choi CS, Chin S, et al. Abnormal glucose homeostasis in skeletal muscle-specific PGC-1 α knockout mice reveals skeletal muscle-pancreatic beta cell crosstalk. *J Clin Invest* 2007;117:3463-3474
- Choi SE, Choi KM, Yoon IH, et al. IL-6 protects pancreatic islet beta cells from pro-inflammatory cytokines-induced cell death and functional impairment *in vitro* and *in vivo*. *Transpl Immunol* 2004;13:43-53
- Franchhauser S, Elias I, Rotter Sopasakis V, et al. Overexpression of Il6 leads to hyperinsulinaemia, liver inflammation and reduced body weight in mice. *Diabetologia* 2008;51:1306-1316
- Andreozzi F, Laratta E, Cardellini M, et al. Plasma interleukin-6 levels are independently associated with insulin secretion in a cohort of Italian-Caucasian nondiabetic subjects. *Diabetes* 2006;55:2021-2024
- Imai J, Katagiri H, Yamada T, et al. Constitutively active PDX1 induced efficient insulin production in adult murine liver. *Biochem Biophys Res Commun* 2005;326:402-409
- Yamada T, Katagiri H, Ishigaki Y, et al. Signals from intra-abdominal fat modulate insulin and leptin sensitivity through different mechanisms: neuronal involvement in food-intake regulation. *Cell Metab* 2006;3:223-229
- Uno K, Katagiri H, Yamada T, et al. Neuronal pathway from the liver modulates energy expenditure and systemic insulin sensitivity. *Science* 2006;312:1656-1659
- Katagiri H, Asano T, Ishihara H, et al. Overexpression of catalytic subunit p110 α of phosphatidylinositol 3-kinase increases glucose transport activity with translocation of glucose transporters in 3T3-L1 adipocytes. *J Biol Chem* 1996;271:16987-16990
- Ishihara H, Takeda S, Tamura A, et al. Disruption of the WFS1 gene in mice causes progressive beta-cell loss and impaired stimulus-secretion coupling in insulin secretion. *Hum Mol Genet* 2004;13:1159-1170
- Imai J, Katagiri H, Yamada T, et al. Regulation of pancreatic beta cell mass by neuronal signals from the liver. *Science* 2008;322:1250-1254
- Imai J, Katagiri H, Yamada T, et al. Cold exposure suppresses serum adiponectin levels through sympathetic nerve activation in mice. *Obesity (Silver Spring)* 2006;14:1132-1141
- Ishigaki Y, Katagiri H, Yamada T, et al. Dissipating excess energy stored in the liver is a potential treatment strategy for diabetes associated with obesity. *Diabetes* 2005;54:322-332
- Harkins JM, Moustaid-Moussa N, Chung YJ, et al. Expression of interleukin-6 is greater in preadipocytes than in adipocytes of 3T3-L1 cells and C57BL/6J and ob/ob mice. *J Nutr* 2004;134:2673-2677
- Brun P, Castagliuolo I, Di Leo V, et al. Increased intestinal permeability in obese mice: new evidence in the pathogenesis of nonalcoholic steatohepatitis. *Am J Physiol Gastrointest Liver Physiol* 2007;292:G518-G525
- Li M, Kim DH, Tsenovoy PL, et al. Treatment of obese diabetic mice with a heme oxygenase inducer reduces visceral and subcutaneous adiposity, increases adiponectin levels, and improves insulin sensitivity and glucose tolerance. *Diabetes* 2008;57:1526-1535
- Wallenius V, Wallenius K, Ahrén B, et al. Interleukin-6-deficient mice develop mature-onset obesity. *Nat Med* 2002;8:75-79
- Ropelle ER, Fernandes MF, Flores MB, et al. Central exercise action increases the AMPK and mTOR response to leptin. *PLoS ONE* 2008;3:e3856
- Banks WA, Kastin AJ, Broadwell RD. Passage of cytokines across the blood-brain barrier. *Neuroimmunomodulation* 1995;2:241-248
- Fasshauer M, Kralisch S, Klier M, et al. Adiponectin gene expression and secretion is inhibited by interleukin-6 in 3T3-L1 adipocytes. *Biochem Biophys Res Commun* 2003;301:1045-1050
- Gustafson B, Smith U. Cytokines promote Wnt signaling and inflammation and impair the normal differentiation and lipid accumulation in 3T3-L1 preadipocytes. *J Biol Chem* 2006;281:9507-9516
- Inoue H, Ogawa W, Ozaki M, et al. Role of STAT-3 in regulation of hepatic gluconeogenic genes and carbohydrate metabolism *in vivo*. *Nat Med* 2004;10:168-174
- Petersen EW, Carey AL, Sacchetti M, et al. Acute IL-6 treatment increases fatty acid turnover in elderly humans *in vivo* and in tissue culture *in vitro*. *Am J Physiol Endocrinol Metab* 2005;288:E155-E162
- Itoh Y, Kawamata Y, Harada M, et al. Free fatty acids regulate insulin secretion from pancreatic beta cells through GPR40. *Nature* 2003;422:173-176
- Ishihara H, Asano T, Tsukuda K, et al. Pancreatic beta cell line MIN6 exhibits characteristics of glucose metabolism and glucose-stimulated insulin secretion similar to those of normal islets. *Diabetologia* 1993;36:1139-1145
- Gilon P, Henquin JC. Mechanisms and physiological significance of the cholinergic control of pancreatic beta-cell function. *Endocr Rev* 2001;22:565-604
- Boulton TG, Stahl N, Yancopoulos GD. Ciliary neurotrophic factor/leukemia inhibitory factor/interleukin 6/oncostatin M family of cytokines induces tyrosine phosphorylation of a common set of proteins overlapping those induced by other cytokines and growth factors. *J Biol Chem* 1994;269:11648-11655
- Lee YH, Bae SS, Seo JK, Choi I, Ryu SH, Suh PG. Interleukin-6-induced tyrosine phosphorylation of phospholipase C- γ 1 in PC12 cells. *Mol Cells* 2000;10:469-474
- Fujiwara K, Maekawa F, Yada T. Oleic acid interacts with GPR40 to induce Ca²⁺ signaling in rat islet beta-cells: mediation by PLC and L-type Ca²⁺ channel and link to insulin release. *Am J Physiol Endocrinol Metab* 2005;289:E670-E677

36. Kelley GG, Zawulich KC, Zawulich WS. Synergistic interaction of glucose and neurohumoral agonists to stimulate islet phosphoinositide hydrolysis. *Am J Physiol* 1995;269:E575–E582
37. Gasa R, Trinh KY, Yu K, Wilkie TM, Newgard CB. Overexpression of G11alpha and isoforms of phospholipase C in islet beta-cells reveals a lack of correlation between inositol phosphate accumulation and insulin secretion. *Diabetes* 1999;48:1035–1044
38. Light PE, Manning Fox JE, Riedel MJ, Wheeler MB. Glucagon-like peptide-1 inhibits pancreatic ATP-sensitive potassium channels via a protein kinase A- and ADP-dependent mechanism. *Mol Endocrinol* 2002;16:2135–2144
39. Ahrén B. Islet G protein-coupled receptors as potential targets for treatment of type 2 diabetes. *Nat Rev Drug Discov* 2009;8:369–385
40. Tsuboi T, da Silva Xavier G, Holz GG, Jouaville LS, Thomas AP, Rutter GA. Glucagon-like peptide-1 mobilizes intracellular Ca^{2+} and stimulates mitochondrial ATP synthesis in pancreatic MIN6 beta-cells. *Biochem J* 2003;369:287–299
41. Teramoto S, Yamamoto H, Ouchi Y. Increased plasma interleukin-6 is associated with the pathogenesis of obstructive sleep apnea syndrome. *Chest* 2004;125:1964–1965
42. Rebecchi MJ, Pentylala SN. Structure, function, and control of phosphoinositide-specific phospholipase C. *Physiol Rev* 2000;80:1291–1335
43. Carey AL, Bruce CR, Sacchetti M, et al. Interleukin-6 and tumor necrosis factor-alpha are not increased in patients with type 2 diabetes: evidence that plasma interleukin-6 is related to fat mass and not insulin responsiveness. *Diabetologia* 2004;47:1029–1037
44. Le Stunff C, Bougnères P. Early changes in postprandial insulin secretion, not in insulin sensitivity, characterize juvenile obesity. *Diabetes* 1994;43:696–702
45. Dubuc PU. The development of obesity, hyperinsulinemia, and hyperglycemia in ob/ob mice. *Metabolism* 1976;25:1567–1574
46. Blonz ER, Stern JS, Curry DL. Dynamics of pancreatic insulin release in young Zucker rats: a heterozygote effect. *Am J Physiol* 1985;248:E188–E193
47. Utzschneider KM, Prigeon RL, Carr DB, et al. Impact of differences in fasting glucose and glucose tolerance on the hyperbolic relationship between insulin sensitivity and insulin responses. *Diabetes Care* 2006;29:356–362
48. Di Gregorio GB, Hensley L, Lu T, Ranganathan G, Kern PA. Lipid and carbohydrate metabolism in mice with a targeted mutation in the IL-6 gene: absence of development of age-related obesity. *Am J Physiol Endocrinol Metab* 2004;287:E182–E187
49. Katagiri H, Yamada T, Oka Y. Adiposity and cardiovascular disorders: disturbance of the regulatory system consisting of humoral and neuronal signals. *Circ Res* 2007;101:27–39
50. Filkins JP. Phases of glucose dyshomeostasis in endotoxemia. *Circ Shock* 1978;5:347–355
51. Yelich MR. Effects of naloxone on glucose and insulin regulation during endotoxemia in fed and fasted rats. *Circ Shock* 1988;26:273–285

Pin1 Associates with and Induces Translocation of CRTC2 to the Cytosol, Thereby Suppressing cAMP-responsive Element Transcriptional Activity^{*S}

Received for publication, April 26, 2010, and in revised form, July 9, 2010. Published, JBC Papers in Press, July 30, 2010, DOI 10.1074/jbc.M110.137836

Yusuke Nakatsu,^{a1} Hideyuki Sakoda,^{b1} Akifumi Kushiya,^c Hiraku Ono,^b Midori Fujishiro,^b Nanao Horike,^d Masayasu Yoneda,^a Haruya Ohno,^a Yoshihiro Tsuchiya,^a Hideaki Kamata,^a Hidetoshi Tahara,^e Toshiaki Isobe,^f Fusanori Nishimura,^g Hideki Katagiri,^h Yoshitomo Oka,^h Toshiaki Fukushima,^a Shin-Ichiro Takahashi,ⁱ Hiroki Kurihara,^d Takafumi Uchida,^j and Tomoichiro Asano^{a2}

From the ^aDepartment of Medical Science, Graduate School of Medicine, University of Hiroshima, 1-2-3 Kasumi, Minami-ku, Hiroshima City, Hiroshima 734-8553, Japan, the Departments of ^bInternal Medicine and ^dPhysiological Chemistry and Metabolism, Graduate School of Medicine, and the ⁱDepartment of Applied Biological Chemistry, Graduate School of Agricultural and Life Sciences, University of Tokyo, 7-3-1 Hongo, Bunkyo-ku, Tokyo 113-0033, Japan, the ^cInstitute for Adult Disease, Asahi Life Foundation, Tokyo 100-0006, Japan, the ^eDepartment of Cellular and Molecular Biology, Graduate School of Biomedical Sciences, Hiroshima University, Hiroshima 734-8553, Japan, the ^fCenter for Priority Areas, Tokyo Metropolitan University, Hachioji, Tokyo 192-0397, Japan, the ^gDepartment of Dental Science for Health Promotion, Hiroshima University Graduate School of Biomedical Sciences, Hiroshima 734-8553, Japan, the ^hDivision of Molecular Metabolism and Diabetes, Tohoku University Graduate School of Medicine, 2-1 Seiryomachi, Aoba-ku, Sendai 980-8575, Japan, and the ^jDepartment of Molecular Cell Biology, Graduate School of Agricultural Science, Tohoku University, Sendai, Miyagi 981-8555, Japan

Pin1 is a unique regulator, which catalyzes the conversion of a specific phospho-Ser/Thr-Pro-containing motif in target proteins. Herein, we identified CRTC2 as a Pin1-binding protein by overexpressing Pin1 with Myc and FLAG tags in mouse livers and subsequent purification of the complex containing Pin1. The association between Pin1 and CRTC2 was observed not only in overexpression experiments but also endogenously in the mouse liver. Interestingly, Ser¹³⁶ in the nuclear localization signal of CRTC2 was shown to be involved in the association with Pin1. Pin1 overexpression in HepG2 cells attenuated forskolin-induced nuclear localization of CRTC2 and cAMP-responsive element (CRE) transcriptional activity, whereas gene knockdown of Pin1 by siRNA enhanced both. Pin1 also associated with CRTC1, leading to their cytosol localization, essentially similar to the action of CRTC2. Furthermore, it was shown that CRTC2 associated with Pin1 did not bind to CREB. Taken together, these observations indicate the association of Pin1 with CRTC2 to decrease the nuclear CBP-CRTC-CREB complex. Indeed, adenoviral gene transfer of Pin1 into diabetic mice improved hyperglycemia in conjunction with normalizing phosphoenolpyruvate carboxykinase mRNA expression levels, which is regulated by CRE transcriptional activity. In conclusion, Pin1 regulates CRE transcriptional activity, by associating with CRTC1 or CRTC2.

Pin1 was initially cloned as a NIMA kinase-interacting protein (1). Since its discovery, numerous proteins have been iden-

tified as Pin1 substrates, including p53, cyclin D1, and Tau (2–5). Pin1 interacts with a number of target proteins through recognition of phospho-Ser/Pro motifs, and the proline conformational change induced by Pin1 modifies the structures and functions, such as stabilization, phosphorylation, and translocation, of target proteins (4–7). Pin1 possesses the WW and PPIase³ domains in its N-terminal (amino acids 1–38) and C-terminal (amino acids 39–163) regions, respectively. To date, many reports have supported an important role for Pin1 in diseases such as cancer and Alzheimer disease (4, 5). In this study, we demonstrated that Pin1 is also involved in metabolic disease via regulation of CRTC2 (CREB-regulated transcriptional co-activator 2; also known as TORC).

The cAMP-responsive element (CRE)-binding protein (CREB) stimulates transcriptional activity through recruitment of the histone acetylase CBP and through an association with CRTC, leading to formation of the CREB-CBP-CRTC complex on a CRE site (8–16). Thus, multiple molecular mechanisms affect the CREB-CBP-CRTC complex, resulting in the regulation of CRE transcriptional activity. They include the phosphorylations of CREB at Ser¹³³, CBP at Ser⁴³⁶, and CRTC2 at Ser¹⁷¹ (16, 17). The phosphorylation of CRTC2 at Ser¹⁷¹ reportedly leads to an association with 14-3-3 protein and thereby to its nuclear exclusion and degradation (16).

The CRTC family consists of three members, CRTC1, CRTC2, and CRTC3 (16, 18). CRTC1 is highly expressed in the brain, whereas the other two are ubiquitously expressed (19). In the liver, insulin induces the phosphorylation of CRTC2 at Ser¹⁷¹, and this phosphorylation leads to the aforementioned

^{*} This work was supported in part by Grant-in-aid for Young Scientists 20790648 (to Y. N.) from the Ministry of Education, Science, Sports, and Culture, Japan.

^S The on-line version of this article (available at <http://www.jbc.org>) contains supplemental Figs. 1–8.

¹ These authors contributed equally to this work.

² To whom correspondence should be addressed. Tel.: 81-82-257-5135; Fax: 81-82-257-5136; E-mail: asano-ty@umin.ac.jp.

³ The abbreviations used are: PPIase, peptidyl-prolyl *cis/trans*-isomerase; CRE, cAMP-response element; CREB, CRE-binding protein; NLS, nuclear localization signal; MEF, mouse embryo fibroblast; STZ, streptozotocin; PEPCK, phosphoenolpyruvate carboxykinase; CRTC, CREB-regulated transcriptional co-activator.

association with 14-3-3 protein and the nuclear exclusion and degradation of CRTC2 (16, 20). In contrast, glucagon induces dephosphorylation of CRTC2 and translocation from the cytosol to the nucleus, thereby forming the CREB·CBP·CRTC2 complex and inducing gluconeogenesis (21). Thus, CRTC2 plays important roles in hepatic glucose metabolism.

In this study, we identified CRTC2 as a Pin1-binding protein. Interestingly, the portion of CRTC2 responsible for the association with Pin1 was revealed to be in the nuclear localization signal (NLS) domain. Herein, we demonstrate that Pin1 regulates the functions and subcellular localizations of CRTC family proteins, thereby altering CRE transcriptional activity.

EXPERIMENTAL PROCEDURES

Materials—Anti-Pin1 antibody was generated by immunizing rabbits with the peptide QMQKPFEDASFATRTGEMSGPVFTDSGIHIITRTE (amino acids 129–163 of human Pin1). Anti-FLAG tag and Myc tag antibodies were purchased from Sigma-Aldrich. The antibodies against CRTC2, CREB, 14-3-3 protein, GFP, and DsRed were purchased from Cell Signaling Technology. Anti-rabbit HRP antibodies conjugated to horseradish peroxidase were obtained from Amersham Biosciences. Dulbecco's modified Eagle's medium (DMEM) and fetal bovine serum were purchased from Invitrogen. All other reagents were of analytical grade.

Preparation of Adenoviruses Expressing MEF-tagged Pin1, CRTC1, and CRTC2—The Myc-TEV-FLAG (MEF) tag cassette was generated by DNA synthesis and inserted into cloning sites in the mammalian expression vector pcDNA3 (Invitrogen; termed pcDNA3-MEF), as reported previously (22). To create the N-terminally MEF-tagged Pin1 construct, human Pin1 cDNA was inserted into pcDNA3-MEF. Then the coding portion of MEF-tagged Pin1 was isolated from pcDNA3-MEF-Pin1, and the recombinant adenoviruses containing the cDNA coding for MEF-tagged Pin1 were constructed as described previously (22). Recombinant adenoviruses expressing human Pin1 with the C-terminal HA tag or N-terminal MEF tag were also constructed and used for adenoviral gene transfer to HepG2 cells and mouse liver. Similarly, adenoviruses expressing GFP-tagged CTRC1, CRTC2, and GFP-tagged CRTC2 were prepared. Adenovirus encoding LacZ served as a control, and the adenoviral gene transfer was performed as reported previously (22).

Purification of MEF-tagged Pin1 from Mouse Livers—Recombinant adenovirus expressing MEF-tagged Pin1 was generated, purified, and concentrated using cesium chloride ultracentrifugation as reported previously (22). Adenovirus encoding LacZ served as a control. Male mice, 9 weeks of age, were obtained from the Nippon Bio-Supp. Center (Tokyo, Japan). They were injected, via the tail vein, with adenovirus at a dose of 2.5×10^7 plaque-forming units/g body weight. Four days after adenovirus injection, the mouse livers were removed and lysed in lysis buffer (50 mM Tris-HCl, pH 7.5, 150 mM NaCl, 10% (w/v) glycerol, 100 mM NaF, 10 mM EGTA, 1 mM Na_3VO_4 , 1% (w/v) Triton X-100, 5 μM ZnCl_2 , 2 mM phenylmethylsulfonyl fluoride, 10 $\mu\text{g}/\text{ml}$ aprotinin, and 1 $\mu\text{g}/\text{ml}$ leupeptin). The lysates were centrifuged at $100,000 \times g$ for 20 min at 4 °C. The supernatant was passed through a 5- μm filter, incubated with 150 μl

of Sepharose beads for 60 min at 4 °C and then passed through a 0.65- μm filter. The filtrated supernatant was mixed with 150 μl of anti-Myc-conjugated Sepharose beads for the first immunoprecipitation. After incubation for 90 min at 4 °C, the beads were washed five times with 1.5 ml of TNTG buffer (20 mM Tris-HCl, pH 7.5, 150 mM NaCl, 10% (w/v) glycerol, 0.1% (w/v) Triton X-100), twice with buffer A (20 mM Tris-HCl, pH 7.5, 150 mM NaCl, and 0.1% (w/v) Triton X-100), and finally once with TNT buffer (50 mM Tris-HCl, pH 8.0, 150 mM NaCl, 0.1% (w/v) Triton X-100). The washed beads were incubated with 15 units of TEV protease (Invitrogen) in 150 μl of TNT buffer to release bound materials from the beads. After incubation for 60 min at room temperature, the supernatant was pooled, and the beads were washed twice with 75 μl of buffer A. The resulting supernatants were combined and incubated with 25 μl of FLAG-Sepharose beads for the second immunoprecipitation. After incubation for 60 min at room temperature, the beads were washed three times with 500 μl of buffer A, and proteins bound to the FLAG beads were dissociated by incubation with 1 mM synthetic FLAG peptides in buffer A for 120 min at 4 °C. Approximately 3 μg of protein (0.01% of starting materials) were routinely recovered by this procedure. The samples were electrophoresed and subjected to SDS-PAGE and immunoblotting.

Cell Culture—Sf9 cells were grown in TC100 (Invitrogen) medium containing 10% fetal calf serum at 27 °C. HepG2 hepatoma cells were grown in DMEM containing 10% fetal calf serum at 37 °C in 5% (v/v) CO_2 in air.

Preparation of Baculoviruses Expressing Pin1 and CRTC2 Constructs—The full-length coding regions of human Pin1, GFP, GFP-tagged Pin1, CRTC2, and DsRed-tagged full-length and various deletion mutant forms of CRTC2 and S136A CRTC2 were subcloned into pBacPAK9 transfer vector (Clontech), and the baculoviruses were prepared according to the manufacturer's instructions. For protein production, Sf9 cells were infected with these baculoviruses and grown for 48 h.

Preparation of Glutathione S-Transferase (GST)-Pin1 Fusion Protein—The cDNAs encoding full-length human Pin1, the WW domain of Pin1, and the PPIase domain of Pin1 were subcloned into a pGEX-5X-1 vector (Amersham Biosciences), which was used to transform *Escherichia coli* JM105 (Promega). Transformed cells were grown to an A_{600} of 0.6 in LB medium supplemented with 0.1 mg/ml ampicillin and stimulated for 3 h with 1.0 mM isopropyl- β -D-thiogalactopyranoside. GST fusion proteins were conjugated to glutathione-Sepharose 4B (Amersham Biosciences) and used for GST pull-down experiments.

GST Pull-down—HepG2 cells expressing MEF-CTR2 and its mutants were homogenized with homogenizing buffer (20 mmol/liter Tris/HCl (pH 7.4), 1% Triton X-100, 0.25% sodium deoxycholate, 0.25 mol/liter NaCl) containing 0.2 mmol/liter phenylmethylsulfonyl fluoride and 5 $\mu\text{g}/\text{ml}$ aprotinin and centrifuged at 15,000 rpm for 30 min at 4 °C, and the supernatants were then recentrifuged at $100,000 \times g$ for 1 h. The supernatants (2 $\mu\text{g}/\text{ml}$ protein concentration) were incubated with 1 ml of glutathione-Sepharose 4B for 1 h at 4 °C to remove nonspecifically bound proteins and then incubated with purified GST alone, GST-Pin1, and GST-Pin1 deletion mutant proteins for 1 h and finally washed six times with homogenizing buffer. glutathione-Sepharose 4B beads

Pin1 Binds to CRTC2 and Suppresses CRE Activity

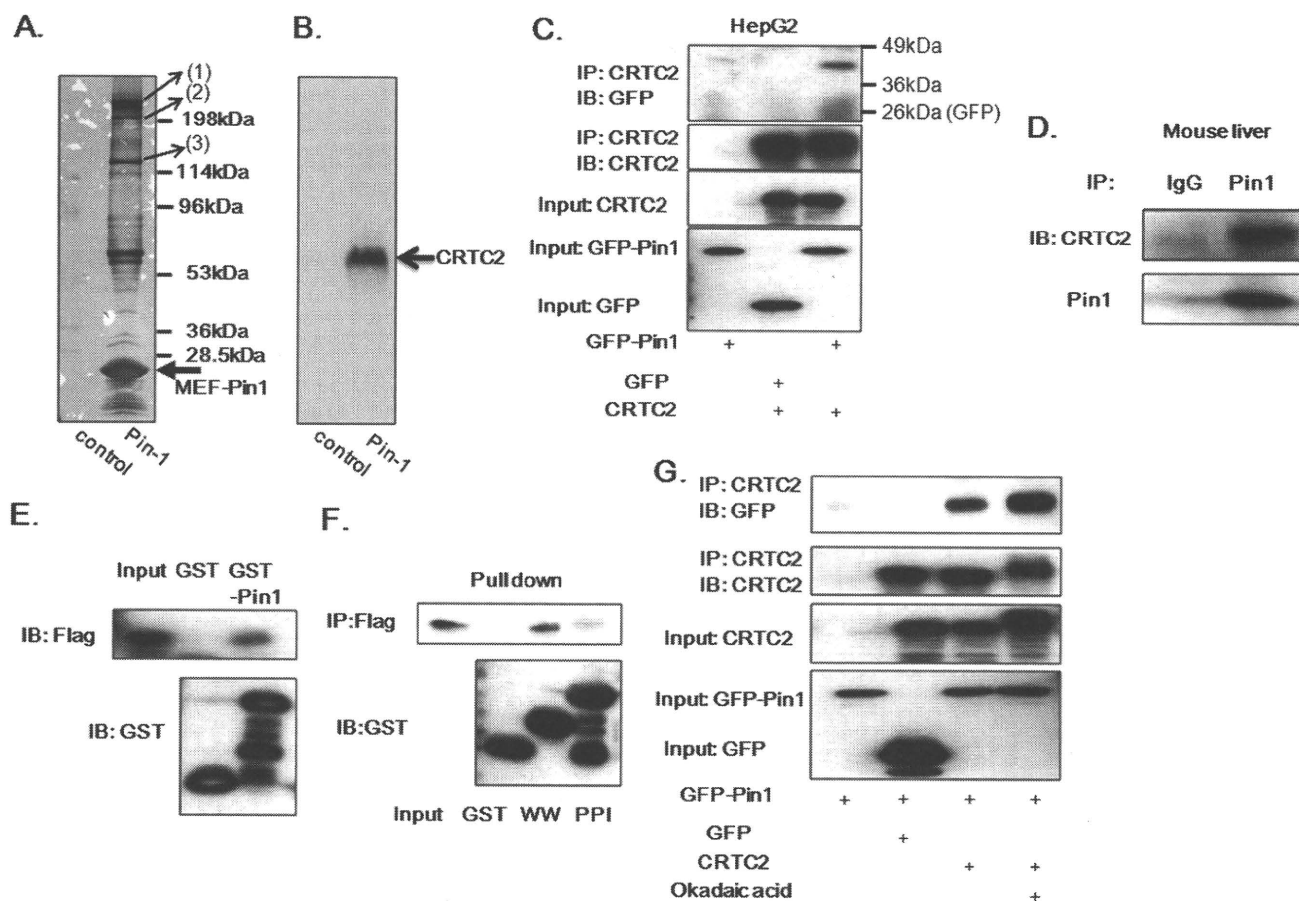


FIGURE 1. Pin1 associates with CRTC2. *A* and *B*, Pin1 with the N-terminal MEF tag was overexpressed in the mouse liver using adenovirus gene transfer, and the Pin1-containing complex was purified. The samples were electrophoresed and subjected to silver staining (*A*). Analysis using LC/MS revealed: *Band (1)*, DNA-directed RNA polymerase II A; *Band (2)*, suppressor of Ty 6 homolog + DNA-directed RNA polymerase II A; *Band (3)*, DNA-directed RNA polymerase II polypeptide B + DNA-directed RNA polymerase I. *B*, the samples were subjected to the immunoblotting with anti-CRTC2 antibody. *C*, CRTC2 or control LacZ was overexpressed with GFP or GFP-Pin1. Then the cell lysates were immunoprecipitated (IP) with anti-CRTC2 antibody, followed by immunoblotting (IB) with anti-GFP antibody. *D*, the cell lysates from the mouse liver were immunoprecipitated with control IgG or anti-Pin1, and the immunoprecipitates were then immunoblotted with anti-CRTC2 and anti-Pin-1. *E*, HepG2 cell lysates expressing CRTC2 with a FLAG tag were incubated with glutathione beads conjugated with GST or GST-Pin1. After washing the beads, SDS-PAGE was performed followed by immunoblotting with anti-FLAG or anti-GST antibodies. *F*, HepG2 cell lysates expressing CRTC2 with a FLAG tag were incubated with glutathione beads conjugated with GST, the GST-WW domain, or the GST-PPI domain. After washing the beads, SDS-PAGE was performed, followed by immunoblotting with anti-FLAG or anti-GST antibodies. *G*, CRTC2 and either GFP or GFP-Pin1 were simultaneously overexpressed in HepG2 cells. With or without okadaic acid treatment for 0.5 h, the cell lysates were immunoprecipitated with anti-CRTC2, followed by immunoblotting with anti-GFP antibody. Representative immunoblotting data from three independent experiments are shown.

were boiled in Laemmli sample buffer, which was used for the SDS-PAGE and immunoblotting.

Preparation of Streptozotocin-treated Diabetic Mice and Gene Transfer of Pin1 into Mouse Livers—Streptozotocin (STZ)-treated diabetic male C57BL/6 mice (8–10 weeks of age) were prepared as reported previously (20). These mice were injected, via the tail vein, with adenovirus at a dose of 2.5×10^7 plaque-forming units/g body weight. Animals were fasted for 14 h and then were refed for 4 h before sacrifice. Blood glucose was measured with a portable blood glucose monitor, Glutest-Ace (Sanwa Kagaku Kenkyusho, Nagoya, Japan). All animal studies were conducted according to the Japanese guidelines for the care and use of experimental animals.

Immunoprecipitation and Immunoblotting—For the immunoprecipitation experiments, whole-cell extracts from HepG2 or Sf9 cells or mouse liver lysates obtained after an overnight fast were prepared in lysis buffer, as described above. Cell or tissue extracts were incubated for 4 h at 4 °C with the indicated antibody and then for 1 h with 30 μ l of protein G-Sepharose

beads. The pellets were washed five times with 1 ml of lysis buffer and then resuspended in Laemmli sample buffer, boiled for 3 min, and analyzed on SDS-polyacrylamide gels.

Western blot analysis was carried out as described previously (22). In brief, 10 μ g of protein were separated by SDS-PAGE and electrophoretically transferred to polyvinylidene difluoride membranes in a transfer buffer consisting of 20 mM Tris-HCl, 150 mM glycine, and 20% methanol. The membranes were blocked with 5% nonfat dry milk in Tris-buffered saline with 0.1% Tween 20 and incubated with specific antibodies, followed by incubation with horseradish peroxidase-conjugated secondary antibodies. The antigen-antibody interactions were visualized by incubation with ECL chemiluminescence reagent (Amersham Biosciences).

Immunostaining—HepG2 cells were fixed with 4% paraformaldehyde for 10 min, rinsed with phosphate-buffered saline (PBS), and then exposed to 0.2% Triton X-100 in PBS for 5 min. Cells were subsequently incubated for 1 h at room temperature with anti-rabbit CRTC2 (1:500), and fluorescein isothiocya-

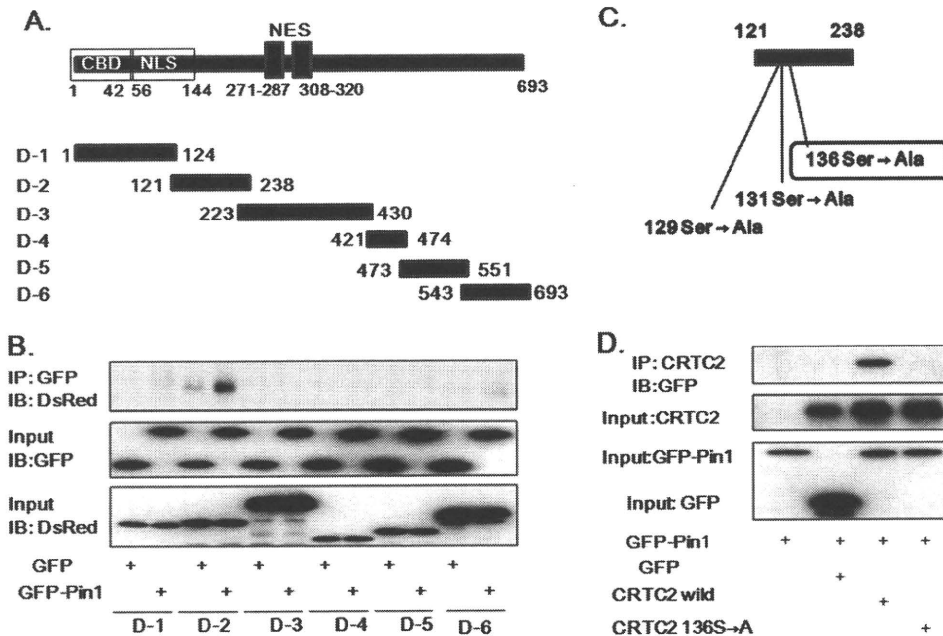


FIGURE 2. Pin1 associates with the NLS domain of CRTC2. *A*, the constructs of CRTC2 deletion mutants and baculoviruses expressing these six mutants with the C-terminal DsRed tag were prepared. *B*, the six deletion mutants with C-terminal DsRed tags were overexpressed with GFP or GFP-Pin1 in Sf9 cells. The cell lysates were immunoprecipitated (IP) with anti-GFP antibody, followed by immunoblotting (IB) with anti-DsRed antibody. The upper panel shows the binding of the Deletion-2 mutant to GFP-Pin1 but not to GFP alone. The orientations of three candidate Ser/Pro motifs in the Deletion-2 mutant involved in the association with Pin1. *D*, wild-type CRTC2 or CRTC2 S136A was overexpressed with GFP-Pin1 or GFP in Sf9 cells. The cell lysates were immunoprecipitated with anti-CRTC2 antibody followed by immunoblotting with anti-GFP. The upper panel shows that CRTC2 S136A does not associate with Pin1, unlike the wild-type CRTC2. Representative immunoblotting data from three independent experiments are shown.

nate-labeled anti-rabbit IgG (1:750) was used as the secondary antibody. Immunofluorescence was visualized with a laser-scanning confocal imaging system.

Luciferase Assay—The following plasmids were obtained from commercial sources: pTAL and pTAL-CRE from Clontech (Palo Alto, CA), pM from Stratagene (La Jolla, CA), and pGL4 and pRL-TK from Promega (Madison, WI). HepG2 cells in a 24-well collagen-coated plate were co-transfected with pTAL-CRE vector (0.25 μ g/well) with an internal reporter, pRL-TK (0.25 μ g). Luciferase activities were determined using the Dual-Luciferase Reporter Assay System (Promega Corp.).

RNA Analysis—RNA extractions were carried out using TRIzol, followed by purification over a QIAEASY RNA column. Reverse transcription and quantitative PCR were carried out as already described. The primer set for human phosphoenolpyruvate carboxykinase (PEPCK) was GGTTCCCAGGGTG-CATGAAA and CACGTAGGGTGAATCCGTCAG (114 bp), and that for human GAPDH was ACCACAGTCCATGCCAT-CAC and TCCACCACCCTGTTGCTGTA (451 bp).

Chromatin Immunoprecipitation Assay with Anti-CRTC2, CBP, or CREB Antibodies—HepG2 cells with or without forskolin stimulation were immunoprecipitated with anti-CRTC2, anti-CBP, or anti-CREB antibody, using the Chip-ITTM express enzymatic kit (Active Motif Corp.). Then precipitated DNA was amplified by PCR using primers against the relevant promoters.

Statistical Analysis—Results are expressed as means \pm S.E., and significance was assessed using one-way analysis of variance unless otherwise indicated.

RESULTS

Identification of CRTC2 in the Pin1-containing Complex from Mouse Liver—The adenovirus to MEF-tagged Pin1 was introduced into mice, and the Pin1-containing complex was purified. Purified Pin1 in the complex was electrophoresed and subjected to silver staining, which showed the presence of Pin1 bait proteins and many binding proteins (Fig. 1A). Bands (1), (2), and (3) were identified to be DNA-directed RNA polymerase II A, DNA-directed RNA polymerase IIB, and DNA-directed RNA polymerase I by the analysis using LC/MS, which agree with previous reports (23). Then we performed the immunoblotting using many antibodies to detect another protein included in the Pin1-containing complex because many faint bands were visible with silver staining.

Many transcriptional co-activators are included among the target proteins of Pin1 (4, 5). In addition, although one of the regulatory mechanisms of Pin1 is protein stabilization, recent reports have shown that Pin1 is involved in translocation of target proteins, such as Bax (24). These results suggest that CRTC2 is a candidate Pin1 target protein because CRTC2 is a transcriptional co-activator and is translocated between the cytosol and the nucleus. As a result, immunoblotting using anti-CRTC2 antibody indicated the presence of CRTC2 in the Pin1 complexes (Fig. 1B). To confirm the association between CRTC2 and Pin1, CRTC2 and each GFP-Pin1 or GFP were simultaneously overexpressed in HepG2 and Sf9 cells. As shown in Fig. 1C and supplemental Fig. 1, GFP-Pin1, but not GFP alone was detected in the anti-CRTC2 immunoprecipitate. Furthermore, CRTC2 was detected in the immunoprecipitate with anti-Pin1 antibody but not that with the control IgG from mouse liver (Fig. 1D). Thus, the association between CRTC2 and Pin1 is physiological.

Pin1 possesses the WW and PPIase domains in its N terminus (amino acids 1–38) and C terminus (amino acids 39–163), respectively. To identify the domain of Pin1 responsible for the association with CRTC2, we prepared GST-Pin1, the GST-Pin1 WW domain, and the GST-Pin1 PPIase domain. These GST proteins were conjugated to beads, followed by incubation with cell lysates from MEF-tagged CRTC2 overexpressing HepG2 cells. GST-Pin1 but not GST alone bound to CRTC2 *in vitro* (Fig. 1E). Using this pull-down system, it was shown that the GST-WW domain, but not the GST-PPIase domain, binds to CRTC2 (Fig. 1F). In addition, okadaic acid treatment significantly increased the association of CRTC2 with Pin1 (Fig. 1G),

Pin1 Binds to CRTC2 and Suppresses CRE Activity

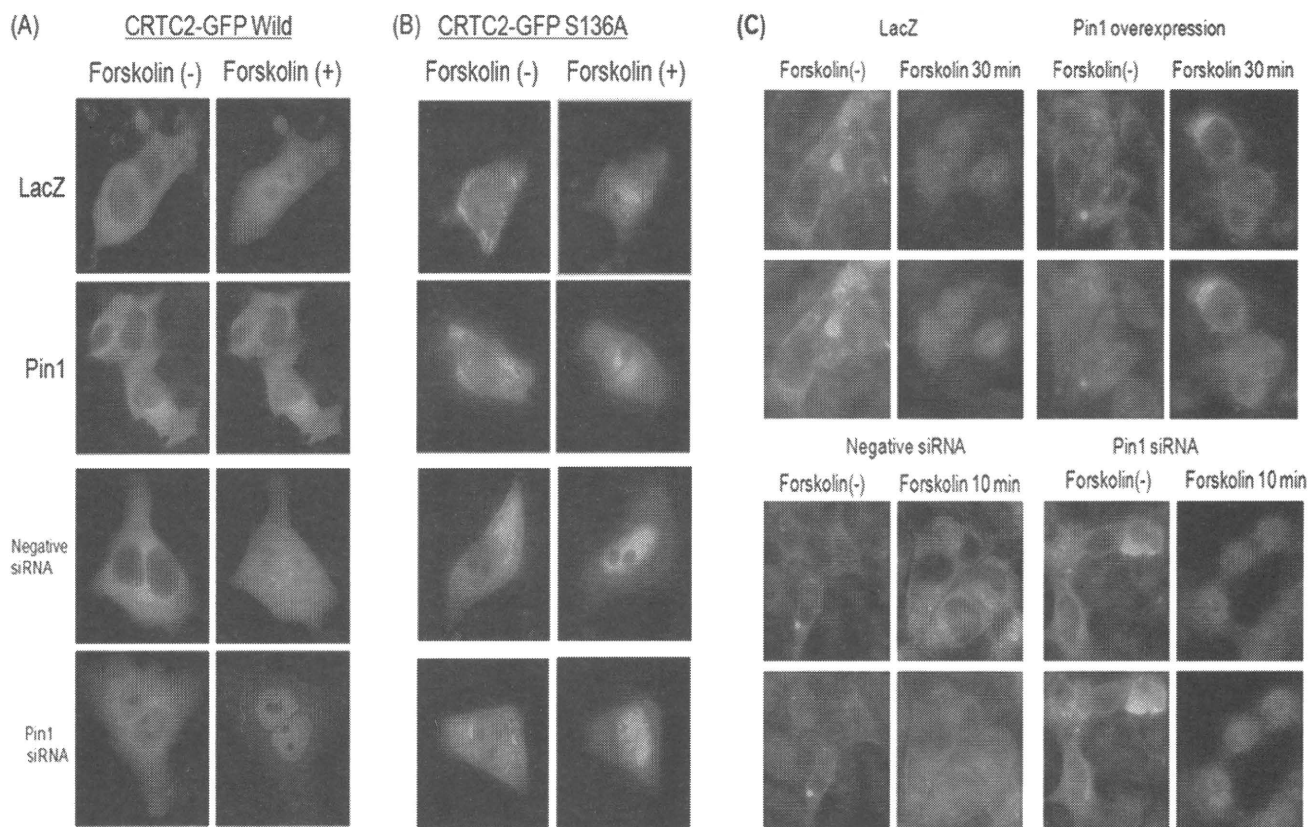


FIGURE 3. Effect of Pin1 on subcellular localization of GFP-tagged CRTC2. *A* and *B*, LacZ or Pin1 was overexpressed, or HepG2 cells were treated with control or Pin1 siRNAs. Then GFP-tagged CRTC2 was overexpressed in HepG2 cells. These cells were treated with forskolin, and the subcellular localization of GFP-tagged wild type or S136A CRTC2 was examined at the indicated periods after initiating forskolin stimulation. Representative data from four independent experiments are shown. *C*, LacZ or Pin1 was overexpressed in HepG2 cells, or the cells were treated with control or Pin1 siRNAs. These cells were treated with forskolin, and the subcellular localization of endogenous CRTC2 was determined by immunostaining at 10 or 30 min after initiating forskolin stimulation. Nuclei were stained with DAPI. Representative data from five independent experiments are shown.

suggesting the involvement of serine and/or threonine phosphorylation(s) in CRTC2.

Pin1 Associates with Ser¹³⁶-containing Motif in the NLS Domain of CRTC2—Subsequently, to reveal the domain of CRTC2 responsible for the association with Pin1, six Ds-Red-tagged CRTC2 N terminus deletion mutants (Fig. 2*A*) and GFP-tagged Pin1 were simultaneously overexpressed in Sf9 cells. As shown in Fig. 2*B*, CRTC2 deletion mutant 2 (D-2), containing amino acids 121–238, was immunoprecipitated with GFP-tagged Pin1 but not with GFP alone. This portion contains three serine-proline motifs (Fig. 2*C*). Each of these serine residues was replaced with alanine, creating a mutant that did not associate with Pin1. As shown in Fig. 2*D*, CRTC2 with serine 136 replaced by alanine did not bind to Pin1, whereas CRTC2 with serine 129 or 131 bound to Pin1 (data not shown). These observations indicated that the association between CRTC2 and Pin1 is mediated via the phosphoserine 136-containing motif in CRTC2 and the WW domain in Pin1. Ser¹³⁶ is in the NLS domain, and a high level of Ser¹³⁶ phosphorylation was demonstrated in a previous report (16).

Pin1 Inhibits CRTC2 Translocation from the Cytosol to the Nucleus—To test whether or not the effect of Pin1 on CRE transcriptional activity is mediated via the effect on the subcellular localization of CRTC2, the GFP-tagged CRTC2 was overexpressed, and the effects of the Pin1 expression level on the subcellular localization of GFP-tagged CRTC2 were analyzed in

the absence or presence of forskolin stimulation (Fig. 3*A*). In the control LacZ-overexpressing or control siRNA-treated HepG2 cells, GFP-tagged CRTC2 was translocated from the cytosol to the nucleus, as reported previously (9). Pin1 overexpression markedly inhibited forskolin-induced translocation of CRTC2 into the nucleus. In addition, gene silencing of Pin1 using siRNA markedly enhanced the nuclear translocation of Pin1 in comparison with treatment with control siRNA. Although nuclear CRTC2 S136A (unable to bind to Pin1) was required for forskolin stimulation, it had no effect on either Pin1 overexpression or Pin1 siRNA (Fig. 3*B*).

In addition, we investigated the effect of Pin1 on the distribution of CRTC2 S171A. CRTC2 S171A (unable to bind to 14-3-3) was mainly present in the nucleus regardless of forskolin stimulation (supplemental Fig. 2). Pin1 overexpression slightly increased CRTC2 S171A in the cytosol, whereas Pin1 siRNA treatment reduced the amount of CRTC2 S171A in the cytosol. This effect of Pin1 was essentially in agreement with the results obtained for wild-type CRTC2.

Similar results were obtained by immunostaining the endogenous CRTC2 in HepG2 cells (Fig. 3*C*). Pin1 overexpression attenuated the forskolin-induced nuclear translocation of CRTC2 as compared with LacZ overexpression. On the other hand, treatment with Pin1 siRNA increased CRTC2 in the nucleus under forskolin stimulation as compared with the control siRNA.

Neither the distribution nor the expression of Pin1 was changed by forskolin or insulin stimulation (supplemental Fig. 3). Thus, a change in Pin1 is not required for regulation of the CRTC2 distribution.

Pin1 Associates with CRTC1 and Induces Its Localization in the Cytosol—The CRTC family consists of three isoforms, CRTC1, CRTC2, and CRTC3. The motif of CRTC2 responsible for the association with Pin1 is present in the NLS and is conserved in CRTC1 but not in CRTC3 (supplemental Fig. 4A). Thus, the associations of Pin1 with CRTC1 were also investigated using HepG2 cells. As shown in supplemental Fig. 4B, FLAG-tagged CRTC1 was detected in anti-GFP immunoprecipitates from the cells expressing GFP-tagged Pin1 and FLAG-tagged CRTC1. As shown in supplemental Fig. 4C, FLAG-tagged CRTC1, in which serine 155 is replaced with alanine, did not bind to GFP-tagged Pin1, unlike the FLAG-tagged wild-type CRTC1.

Then the effects of Pin1 on localizations of CRTC1 were examined. When LacZ was overexpressed, GFP-tagged CRTC1 was present in the cytosol and translocated to the nucleus in response to forskolin stimulation (supplemental Fig. 4D). This translocation was markedly inhibited by Pin1 overexpression (supplemental Fig. 4D).

CRTC2 Associated with Pin1 Did Not Bind to CREB—Formation of the CREB-CBP-CRTC complex, which binds to a CRE site, is critical for CRE transcriptional activation. We investigated whether or not the CREB-CBP-CRTC2-Pin1 complex can form, using the baculovirus and Sf9 cell overexpression system. When CRTC2 and CREB were both overexpressed in HepG2 or Sf9 cells, CREB was detected in the CRTC2 immunoprecipitate. Interestingly, the overexpression of Pin1 markedly reduced the association between CREB and CRTC2, in either HepG2 or Sf9 cells (Fig. 4, A and B).

Furthermore, the effect of Pin1 on the association between CRTC2 and 14-3-3 was investigated. In Sf9 cell lysates overexpressing CREB and CRTC2, both CRTC2 and endogenously expressed 14-3-3 protein were detected in anti-CREB immunoprecipitates (Fig. 4C). In the case of triple overexpressions of CRTC2, CREB, and GFP-tagged Pin1, CRTC2 and 14-3-3 were detectable in the GFP-tagged Pin1 immunoprecipitate (Fig. 4D).

Similar results were obtained in the HepG2 cells. The association between MEF-tagged CRTC2 and endogenously expressed 14-3-3 was not affected by the overexpression of Pin1 (supplemental Fig. 5A). In addition, Pin1 overexpression did not affect the phosphorylation level of Ser¹⁷¹, responsible for the association with 14-3-3, in either basal or forskolin-stimulated conditions (supplemental Fig. 5B). These results suggest that Pin1-associated CRTC2 is capable of binding to 14-3-3 protein but not to CREB.

Pin1 Inhibits CRE Transcriptional Activity and Its Downstream PEPCK Expression—Subsequently, to elucidate the role of Pin1 in CRE transcriptional activity, the effects of Pin1 overexpression and Pin1 gene silencing using siRNA on the CRE and PEPCK luciferase assay, and PEPCK mRNA level were investigated in HepG2 cells (Fig. 5). The amount of overexpressed Pin1 was ~5 times that of endogenous Pin1 in HepG2 cells. Under these conditions, forskolin-induced transcrip-

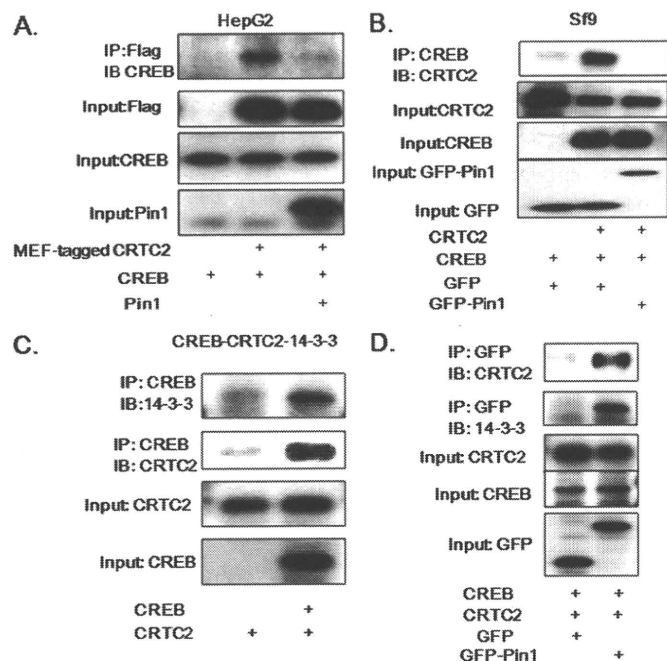


FIGURE 4. Binding of Pin1 to CRTC2 inhibits the association between CREB and CRTC2 but not that between 14-3-3 and CRTC2. A, MEF-tagged CRTC2, CREB, and Pin1 were overexpressed in HepG2 cells in the indicated combinations. The cell lysates were immunoprecipitated (IP) with anti-FLAG antibody and immunoblotted (IB) with anti-CREB antibody. B, CRTC2, CREB, and Pin1 were overexpressed in Sf9 cells in the indicated combinations. The cell lysates were immunoprecipitated with anti-CREB antibody and immunoblotted with anti-CRTC2 antibody. C, CREB and CRTC2 were overexpressed in Sf9 cells. The cell lysates were immunoprecipitated with anti-CREB antibody and immunoblotted with anti-14-3-3 protein antibody. D, CREB, CRTC2, and either GFP or GFP-Pin1 were overexpressed in Sf9 cells. The cell lysates were immunoprecipitated with anti-GFP antibody and immunoblotted with anti-CRTC2 or anti-14-3-3 protein antibody. Representative data from four independent experiments are shown.

tional activity and PEPCK mRNA induction were significantly attenuated (Fig. 5, A–C). On the contrary, gene suppression of Pin1 using siRNA significantly enhanced these events (Fig. 5, D–F). In addition, suppressions of CRE-luciferase and PEPCK-luciferase activities by Pin1 overexpression were observed in immortalized human hepatocytes (supplemental Fig. 6) (25), suggesting that this mechanism is independent of the glucose sensitivity of the cell type. An inhibitory effect of Pin1 on CRE luciferase activity was observed when wild type or S171A CRTC2, but not S136A, was overexpressed, consistent with the results showing Pin1 to regulate the translocation of CRTC2 (supplemental Fig. 7). Thus, the Pin1 expression level was revealed to negatively regulate CRE transcriptional activity.

Chromatin Immunoprecipitation Assay with Anti-CRTC2 and CREB Antibodies—Because Pin1-associated CRTC2 did not bind CREB, we performed a ChIP assay to investigate whether or not Pin1 affected recruitment of CRTC2 to cAMP-responsive elements upstream of PEPCK, NR4A2, and CGA genes (Fig. 5G). The PCR product obtained using the anti-CREB immunoprecipitate was unchanged regardless of forskolin stimulation or Pin1 overexpression. In contrast, the PCR product of the anti-CRTC2 immunoprecipitate was markedly increased by forskolin stimulation, and Pin1 overexpression abolished this increase. Forskolin stimulation induced CBP recruitment to the promoter as well as CRTC2, but Pin1 overexpression had no effect.

Pin1 Binds to CRTC2 and Suppresses CRE Activity

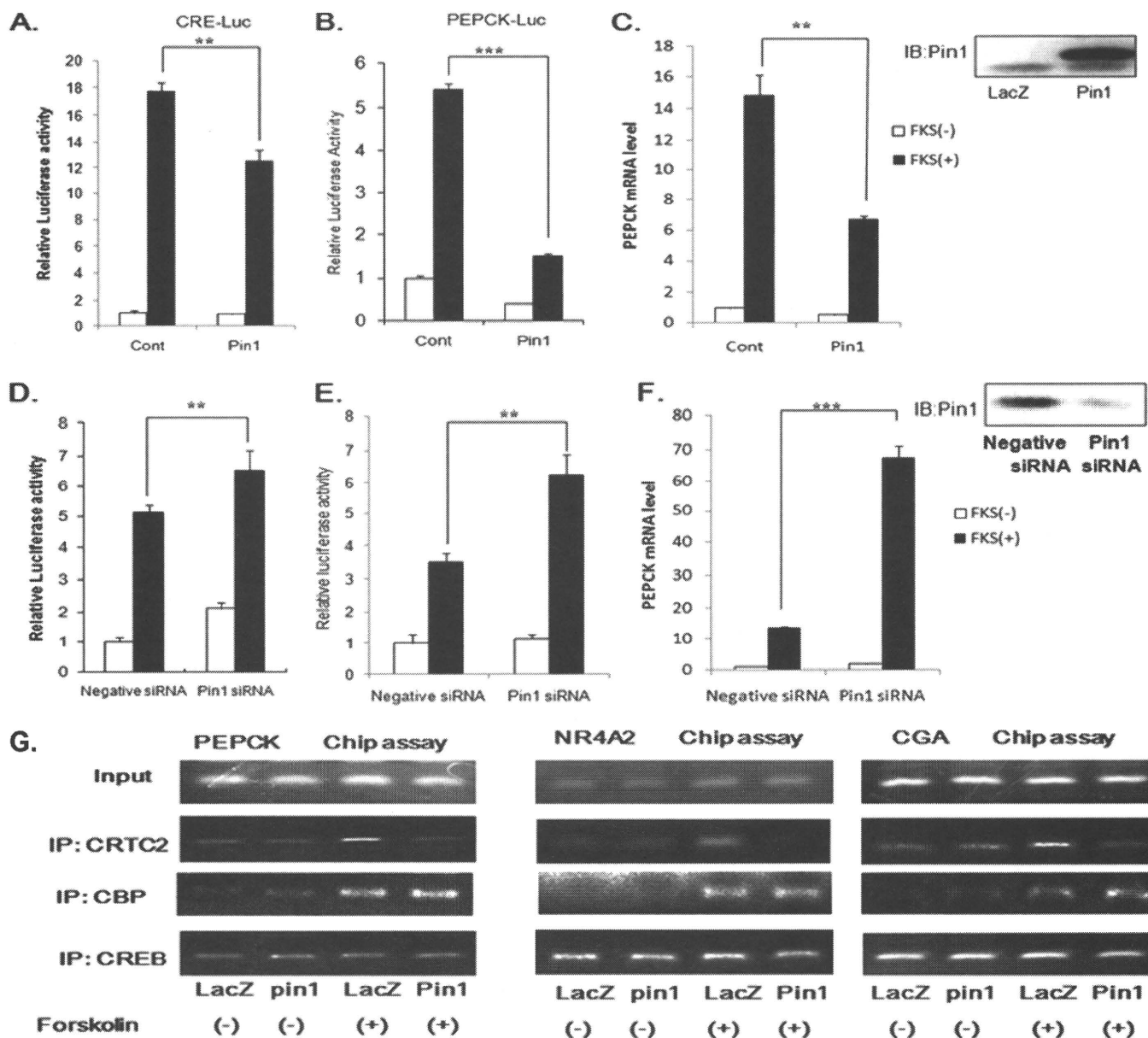


FIGURE 5. Pin1 suppresses CRE luciferase activity and PEPCK mRNA level in HepG2 cells. *A* and *B*, LacZ or Pin1 was overexpressed in HepG2 cells transfected with pTAL and pTAL-CRE or pTAL-PEPCK. *D* and *E*, these transfected HepG2 cells were treated with control siRNA or Pin1 siRNA. In two experiments, with and without forskolin stimulation for 6 h, the cell lysates from HepG2 cells were subjected to the luciferase assay. *C* and *F*, PEPCK mRNA levels were also measured. Representative data from four independent experiments are shown. **, $p < 0.01$ versus LacZ or negative siRNA. *G*, HepG2 cells overexpressing LacZ or Pin1 were subjected to the CHIP assay using anti-CRTC2, anti-CNP, or anti-CREB antibodies and primers corresponding to the PEPCK, NR4A2, and CGA promoter regions. Representative data from four independent experiments are shown. *IB*, immunoblot; *IP*, immunoprecipitation. Error bars, S.E.

Thus, it was suggested that CRTC2 associated with Pin1 was removed from CREB located in the CRE sequence in the PEPCK, NR4A2, and CGA promoter region.

Hepatic Pin1 Overexpression Reduces PEPCK Expression and Decreases Hyperglycemia in STZ-induced Diabetic Mice—CRTC2 is a major transcriptional co-activator for hepatic glucose regulation via its effects on PEPCK expression. Thus, we considered the possibility of the regulation of PEPCK expression by Pin1 in the liver, and an adenovirus expressing Pin1 was introduced into STZ-induced insulin-deficient diabetic mice. Due to the insulin deficiency, as reported previously, hepatic PEPCK mRNA and serum blood glucose levels were markedly increased in fed and fasted state, as compared with the control

mice (Fig. 6). The adenovirus for Pin1 expression was injected intravenously, and 96 h later, overexpressed Pin1 was detected only in the liver (Fig. 6A) and not in other tissues. With Pin1 overexpression in the liver, the increased hepatic PEPCK mRNA level in STZ-mice was normalized, and blood glucose elevation was also partially but significantly reduced in both the fed and the fasting state (Fig. 6, B–E). Pin1 overexpression exerted the same effects on other CRE-dependent transcriptional genes, such as G6Pase, PGC-1 α , and CPT-1. These findings revealed Pin1 to be a regulator of CRE-dependent transcriptional genes *in vivo*.

Pin1 Expression Is Low in Fasting State—Finally, we investigated the changes in Pin1 expressions under different nutrient condi-

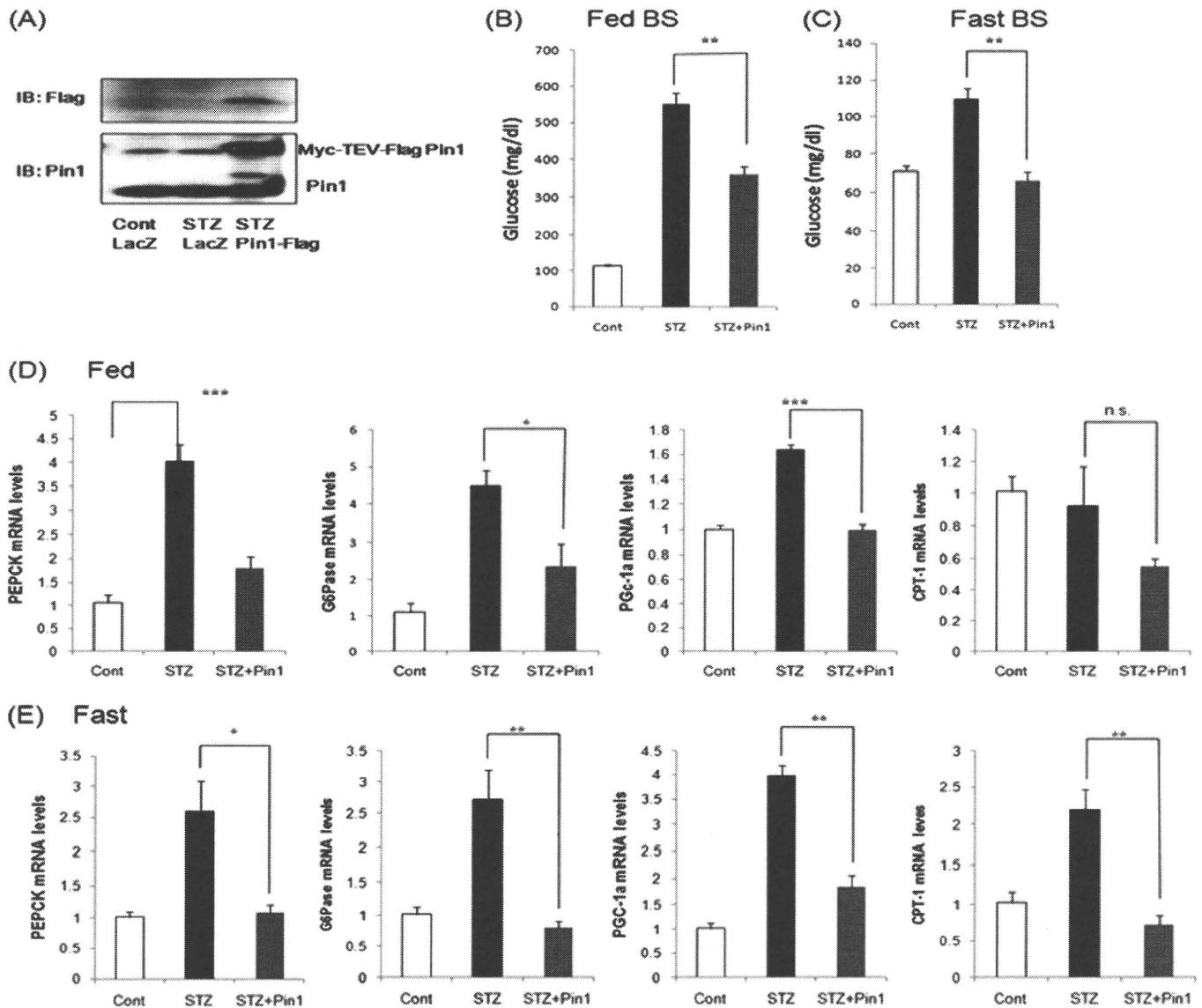


FIGURE 6. Hepatic overexpression of Pin1 restored elevated CRE-dependent transcriptional genes and hyperglycemia in STZ-treated mice. STZ-treated diabetic C57BL/6 male mice were injected with 2.5×10^7 plaque-forming units/g body weight of adenovirus containing β -galactosidase (*LacZ*) or FLAG-tagged Pin1 construct via the tail vein. *A*, immunoblotting of hepatic tissue lysates with anti-FLAG or anti-Pin1 antibody. *B* and *C*, serum glucose concentrations in fed and fasting states ($n = 6$, each group). *D* and *E*, CRE-dependent transcriptional gene mRNA levels in the liver. **, $p < 0.01$ versus STZ; ***, $p < 0.001$ versus STZ. Error bars, S.E.

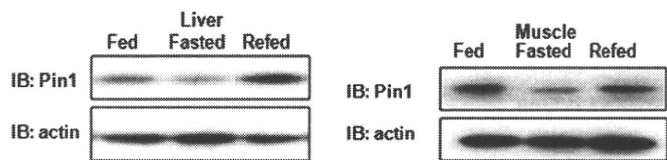


FIGURE 7. Pin1 expression is regulated by nutrient conditions. Mice were fed routinely, starved for 20 h, or refed for 4 h after a 20-h fast. Liver (*left*) and muscle (*right*) cell lysates were prepared and then immunoblotted with anti-Pin1 antibody. A representative immunoblot (IB) is shown in the upper panel.

tions. Interestingly, we found that the Pin1 expression level is low in the fasted state but is increased by feeding (Fig. 7). Thus, Pin1 expression appears to be regulated by nutrient conditions.

DISCUSSION

CRE transcriptional activity is enhanced through association of the CREB·CBP·CRTC complex on a CRE site. The co-activator of CREB termed the CRTC family consists of

three isoforms, CRTC1, CRTC2, and CRTC3 (18). CRTC2 was reported to be important for the regulation of CRE transcriptional activity and its downstream PEPCK gene expression (20). Depletion of nuclear CRTC2 leads to the suppression of CRE transcriptional activity (20). Thus, both the subcellular localization of CRTC2 and CREB·CBP·CRTC complex formation are critical for CRE transcriptional activity. CRTC2 is reportedly phosphorylated by AMPK and SIK, and phosphorylated CRTC2 binds to 14-3-3 protein and is thereby shifted from the nucleus to the cytoplasm (21). The Montminy group (16) has identified 12 independent phosphorylated serine residues on CRTC2 using tandem MS analysis. They demonstrated that PKA inhibits the activity of SIK and reduces Ser¹⁷¹ phosphorylation leading to binding with 14-3-3 protein and translocation to the cytosol (16). However, the importance of other phosphorylation sites identified in their study, such as Ser¹³⁶ remains unknown.

Pin1 Binds to CRTC2 and Suppresses CRE Activity

In this study, it was demonstrated that Pin1 associates with the CRTC family of proteins consisting of CRTC1 and CRTC2. Because the portion of CRTC1 and CRTC2 responsible for the association with Pin1 is in the NLS domain, we considered the possibility that the binding of Pin1 to this portion would interrupt NLS function, resulting in their export from the nucleus. In fact, our observations using GFP-tagged CRTC1 and CRTC2 as well as staining of endogenous CRTC2 supported our hypothesis. On the other hand, gene silencing of Pin1 using siRNA markedly induced nuclear localization of CRTC2 when stimulated with forskolin. It is likely that altered localization of CRTC2 due to Pin1 takes place independently of the binding of 14-3-3 protein to CRTC2 because Pin1 overexpression affected neither the Ser¹⁷¹ phosphorylation level of CRTC2 nor the association with 14-3-3.

A further interesting issue is that CRTC2 associated with Pin1 did not bind to CREB. This phenomenon cannot be attributable to the different subcellular distributions of CREB, CBP, and CRTC because highly overexpressed CREB, CBP, and CRTC2 are present in the cytosol of Sf9 cells. Taken together, these observations indicate the association of Pin1 with CRTC2 to decrease the nuclear CBP·CRTC2·CREB complex via two mechanisms (*i.e.* the export of CRTC2 and interruption of the association between CRTC2 and CREB). Thus, the Pin1 expression level is a key factor regulating CRE transcriptional activity.

We investigated the effects of various kinase inhibitors on the association between CRTC2 and Pin1, using HepG2 cells, in an effort to identify the kinase that is involved in the phosphorylation of S136A on CRTC2. However, we were unable to obtain clear results. Although we did not discover which kinase(s) phosphorylates the Ser¹³⁶ of CRTC2 responsible for the association with Pin1 in this study, high basal phosphorylation of Ser¹³⁶ was already demonstrated in a previous report (16).

Prior studies have also shown that Pin1 expression generally correlates with cell proliferative potential in normal tissues (1, 26, 27) and is further up-regulated in many human cancers (28–31). In addition, interestingly, we noticed that the amount of Pin1 was higher in the fed than in the fasting state, in both liver and muscle. However, neither insulin nor forskolin has any effect on the expression of Pin1 in HepG2. Thus, the mechanism(s) involved in the altered expression of Pin1 remains unclear, although this is an important issue that merits further investigation.

In the liver, CRE transcriptional activity plays a critical role in gluconeogenesis (32–34). In addition, in the diabetic state, insufficient suppression of CRE transcriptional activity is regarded as a mechanism underlying hyperglycemia under fasted conditions (35). In the present study, our final experiment examined whether Pin1 overexpression might improve the hyperglycemia in insulin-deficient STZ-treated mice. In these mice, gluconeogenic enzymes, such as PEPCK, under the control of CRE transcriptional activity are reportedly up-regulated (20, 36, 37) due to insulin deficiency and the relatively increased effect of glucagon. The fact that Pin1 overexpression reduced the high PEPCK expression and its resultant fasting serum glucose elevation in STZ-treated mice suggests that the Pin1 expression level is involved in regulating glucose metabo-

lism. Thus, an agent affecting Pin1 expression or activity may represent a novel therapeutic strategy for diabetes.

To date, numerous proteins have been identified as substrates of Pin1 (4, 5, 38). With the proline conformational change induced by Pin1, the structure and function of the target protein are modified, which affects protein stabilization, subcellular localization, phosphorylation, transcriptional activity, etc. In the case of CRTC2, both subcellular localization and the complex-forming function with CREB are affected.

Although we did not investigate the physiological effects occurring via CRTC1 induced by the association with Pin1, we did observe that Pin1 is highly expressed in the brain, whereas its enzymatic activity is blunted by oxidative stress modification that occurs in the early stages of Alzheimer disease (39). Although the physiological function of Pin1 in neurons remains largely unknown, numerous reports have implicated CRE transcriptional activity in brain function (40–42). Thus, further important evidence may be obtained from studies of Pin1 and CRTC1 in the brain or other tissues.

In summary, CRTC2 was identified as a new Pin1-binding protein. The CBP·CRTC2·CREB complex promotes gluconeogenesis. Pin1 binding to CRTC2 prevents this complex formation, thereby suppressing CRE transcriptional activity (supplemental Fig. 8). These findings indicate that Pin1 is a regulator of gluconeogenesis and may be a new target for diabetic therapy.

REFERENCES

1. Lu, K. P., Hanes, S. D., and Hunter, T. (1996) *Nature* **380**, 544–547
2. Lu, P. J., Wulf, G., Zhou, X. Z., Davies, P., and Lu, K. P. (1999) *Nature* **399**, 784–788
3. Pinton, P., Rimessi, A., Marchi, S., Orsini, F., Migliaccio, E., Giorgio, M., Contursi, C., Minucci, S., Mantovani, F., Wieckowski, M. R., Del Sal, G., Pelicci, P. G., and Rizzuto, R. (2007) *Science* **315**, 659–663
4. Takahashi, K., Uchida, C., Shin, R. W., Shimazaki, K., and Uchida, T. (2008) *Cell Mol. Life Sci.* **65**, 359–375
5. Wulf, G., Finn, G., Suizu, F., and Lu, K. P. (2005) *Nat. Cell Biol.* **7**, 435–441
6. Ranganathan, R., Lu, K. P., Hunter, T., and Noel, J. P. (1997) *Cell* **89**, 875–886
7. Schutkowski, M., Bernhardt, A., Zhou, X. Z., Shen, M., Reimer, U., Rahfeld, J. U., Lu, K. P., and Fischer, G. (1998) *Biochemistry* **37**, 5566–5575
8. Bittinger, M. A., McWhinnie, E., Meltzer, J., Iourgenko, V., Latario, B., Liu, X., Chen, C. H., Song, C., Garza, D., and Labow, M. (2004) *Curr. Biol.* **14**, 2156–2161
9. Dentin, R., Hedrick, S., Xie, J., Yates, J., 3rd, and Montminy, M. (2008) *Science* **319**, 1402–1405
10. He, L., Sabet, A., Djedjos, S., Miller, R., Sun, X., Hussain, M. A., Radovick, S., and Wondisford, F. E. (2009) *Cell* **137**, 635–646
11. Herzig, S., Long, F., Jhala, U. S., Hedrick, S., Quinn, R., Bauer, A., Rudolph, D., Schutz, G., Yoon, C., Puigserver, P., Spiegelman, B., and Montminy, M. (2001) *Nature* **413**, 179–183
12. Jansson, D., Ng, A. C., Fu, A., Depatie, C., Al Azzabi, M., and Sreaton, R. A. (2008) *Proc. Natl. Acad. Sci. U.S.A.* **105**, 10161–10166
13. Lerner, R. G., Depatie, C., Rutter, G. A., Sreaton, R. A., and Balthasar, N. (2009) *EMBO Rep.* **10**, 1175–1181
14. Liu, Y., Dentin, R., Chen, D., Hedrick, S., Ravnskjaer, K., Schenk, S., Milne, J., Meyers, D. J., Cole, P., Yates, J., 3rd, Olefsky, J., Guarente, L., and Montminy, M. (2008) *Nature* **456**, 269–273
15. Radhakrishnan, I., Pérez-Alvarado, G. C., Parker, D., Dyson, H. J., Montminy, M. R., and Wright, P. E. (1997) *Cell* **91**, 741–752
16. Sreaton, R. A., Conkright, M. D., Katoh, Y., Best, J. L., Canetti, G., Jeffries, S., Guzman, E., Niessen, S., Yates, J. R., 3rd, Takemori, H., Okamoto, M., and Montminy, M. (2004) *Cell* **119**, 61–74

17. Zhou, X. Y., Shibusawa, N., Naik, K., Porras, D., Temple, K., Ou, H., Kaihara, K., Roe, M. W., Brady, M. J., and Wondisford, F. E. (2004) *Nat. Med.* **10**, 633–637
18. Iourgenko, V., Zhang, W., Mickanin, C., Daly, I., Jiang, C., Hexham, J. M., Orth, A. P., Miraglia, L., Meltzer, J., Garza, D., Chirn, G. W., McWhinnie, E., Cohen, D., Skelton, J., Terry, R., Yu, Y., Bodian, D., Buxton, F. P., Zhu, J., Song, C., and Labow, M. A. (2003) *Proc. Natl. Acad. Sci. U.S.A.* **100**, 12147–12152
19. Wu, Z., Huang, X., Feng, Y., Handschin, C., Feng, Y., Gullicksen, P. S., Bare, O., Labow, M., Spiegelman, B., and Stevenson, S. C. (2006) *Proc. Natl. Acad. Sci. U.S.A.* **103**, 14379–14384
20. Dentin, R., Liu, Y., Koo, S. H., Hedrick, S., Vargas, T., Heredia, J., Yates, J., 3rd, and Montminy, M. (2007) *Nature* **449**, 366–369
21. Koo, S. H., Flechner, L., Qi, L., Zhang, X., Srean, R. A., Jeffries, S., Hedrick, S., Xu, W., Boussouar, F., Brindle, P., Takemori, H., and Montminy, M. (2005) *Nature* **437**, 1109–1111
22. Sakoda, H., Gotoh, Y., Katagiri, H., Kurokawa, M., Ono, H., Onishi, Y., Anai, M., Ogihara, T., Fujishiro, M., Fukushima, Y., Abe, M., Shojima, N., Kikuchi, M., Oka, Y., Hirai, H., and Asano, T. (2003) *J. Biol. Chem.* **278**, 25802–25807
23. Xu, Y. X., and Manley, J. L. (2007) *Genes Dev.* **21**, 2950–2962
24. Shen, Z. J., Esnault, S., Schinzel, A., Borner, C., and Malter, J. S. (2009) *Nat. Immunol.* **10**, 257–265
25. Tontonoz, P., Hu, E., Devine, J., Beale, E. G., and Spiegelman, B. M. (1995) *Mol. Cell. Biol.* **15**, 351–357
26. Waki, K., Anno, K., Ono, T., Ide, T., Chayama, K., and Tahara, H. (2010) *Cancer Sci.* **101**, 1678–1685
27. Winkler, K. E., Swenson, K. I., Kornbluth, S., and Means, A. R. (2000) *Science* **287**, 1644–1647
28. Ryo, A., Nakamura, M., Wulf, G., Liou, Y. C., and Lu, K. P. (2001) *Nat. Cell Biol.* **3**, 793–801
29. Wulf, G. M., Ryo, A., Wulf, G. G., Lee, S. W., Niu, T., Petkova, V., and Lu, K. P. (2001) *EMBO J.* **20**, 3459–3472
30. Yeh, E., Cunningham, M., Arnold, H., Chasse, D., Monteith, T., Ivaldi, G., Hahn, W. C., Stukenberg, P. T., Shenolikar, S., Uchida, T., Counter, C. M., Nevins, J. R., Means, A. R., and Sears, R. (2004) *Nat. Cell Biol.* **6**, 308–318
31. Zheng, H., You, H., Zhou, X. Z., Murray, S. A., Uchida, T., Wulf, G., Gu, L., Tang, X., Lu, K. P., and Xiao, Z. X. (2002) *Nature* **419**, 849–853
32. Erion, D. M., Ignatova, I. D., Yonemitsu, S., Nagai, Y., Chatterjee, P., Weismann, D., Hsiao, J. J., Zhang, D., Iwasaki, T., Stark, R., Flannery, C., Kahn, M., Carmean, C. M., Yu, X. X., Murray, S. F., Bhanot, S., Monia, B. P., Cline, G. W., Samuel, V. T., and Shulman, G. I. (2009) *Cell Metab.* **10**, 499–506
33. Rhee, J., Inoue, Y., Yoon, J. C., Puigserver, P., Fan, M., Gonzalez, F. J., and Spiegelman, B. M. (2003) *Proc. Natl. Acad. Sci. U.S.A.* **100**, 4012–4017
34. Rodgers, J. T., Lerin, C., Haas, W., Gygi, S. P., Spiegelman, B. M., and Puigserver, P. (2005) *Nature* **434**, 113–118
35. Yoon, J. C., Puigserver, P., Chen, G., Donovan, J., Wu, Z., Rhee, J., Adelman, G., Stafford, J., Kahn, C. R., Granner, D. K., Newgard, C. B., and Spiegelman, B. M. (2001) *Nature* **413**, 131–138
36. Clément, S., Krause, U., Desmedt, F., Tanti, J. F., Behrends, J., Pesesse, X., Sasaki, T., Penninger, J., Doherty, M., Malaisse, W., Dumont, J. E., Le Marchand-Brustel, Y., Erneux, C., Hue, L., and Schurmans, S. (2001) *Nature* **409**, 92–97
37. Fisher, S. J., and Kahn, C. R. (2003) *J. Clin. Invest.* **111**, 463–468
38. Ryo, A., Suizu, F., Yoshida, Y., Perrem, K., Liou, Y. C., Wulf, G., Rottapel, R., Yamaoka, S., and Lu, K. P. (2003) *Mol. Cell.* **12**, 1413–1426
39. Sultana, R., Boyd-Kimball, D., Poon, H. F., Cai, J., Pierce, W. M., Klein, J. B., Markesbery, W. R., Zhou, X. Z., Lu, K. P., and Butterfield, D. A. (2006) *Neurobiol. Aging* **27**, 918–925
40. Bito, H., Deisseroth, K., and Tsien, R. W. (1996) *Cell* **87**, 1203–1214
41. Nibuya, M., Nestler, E. J., and Duman, R. S. (1996) *J. Neurosci.* **16**, 2365–2372
42. Tao, X., Finkbeiner, S., Arnold, D. B., Shaywitz, A. J., and Greenberg, M. E. (1998) *Neuron* **20**, 709–726

Efficacy and safety of patient-directed titration of once-daily pre-dinner premixed biphasic insulin aspart 70/30 injection in Japanese type 2 diabetic patients with oral antidiabetic drug failure: STEP-AKITA study

Takuma Narita^{1*}, Takashi Goto², Yumi Suganuma^{1,2}, Mihoko Hosoba^{1,3}, Tsukasa Morii¹, Takehiro Sato¹, Hiroki Fujita¹, Takeshi Miura^{1,3}, Takashi Shimotomai^{4,5}, Yuichiro Yamada¹, Masafumi Kakei^{1,6}

ABSTRACT

Aims/Introduction: To clarify clinical characteristics related to optimal glycaemic control achieved after adding once-daily pre-dinner biphasic insulin aspart 70/30 (BIAsp 30) in Japanese type 2 diabetic (T2D) patients with oral antidiabetic drug (OAD) failure.

Materials and Methods: Under this regimen, we evaluated changes in HbA_{1c} levels and daily self-monitoring blood glucose (BG) profiles, as well as the incidences of hypoglycaemia and retinopathy progression. The patients adjusted BIAsp 30 dosages themselves every 3–4 days according to a pre-determined algorithm to achieve fasting BG levels of 101–120 mg/dL. HbA_{1c} levels were expressed as Japan Diabetes Society values.

Results: Of 29 enrolled patients, 22 (HbA_{1c} levels, 8.5 ± 1.5% [mean ± SD]) and 20 patients completed the 16- and 24-week follow-up, respectively. At 16 weeks 68.2 and 45.5%, and at 24 weeks 80.0 and 35% of patients had achieved HbA_{1c} levels of <7.0 and <6.5%, respectively. The patients who had achieved optimal glycaemic control, including daytime postprandial BG profiles after treatment, had lower post-breakfast BG excursions at baseline, shorter diabetes durations and younger age. No severe hypoglycaemic episodes were recorded. Progression of retinopathy was observed in 3 of the 29 enrolled patients.

Conclusions: Lower post-breakfast BG excursions, shorter diabetes duration and younger age in Japanese T2D patients with OAD failure might warrant optimal glycaemic control with safety after adding once-daily pre-dinner BIAsp 30 initiating regimen. (*J Diabetes Invest*, doi: 10.1111/j.2040-1124.2010.00062.x, 2010)

KEY WORDS: Biphasic insulin aspart 70/30, Insulin initiation, Self-adjusted treatment algorithm

INTRODUCTION

To reduce the risk of diabetic chronic complications, it is crucial to achieve ideal glycaemic control as early as possible in diabetic patients^{1–4}. In clinical practice, under recent guidelines, a HbA_{1c} level of <6.5–7.0% is recommended as the target for glycaemic control in diabetic patients^{5,6}.

The progressive decline in β -cell function in type 2 diabetic (T2D) patients has been reported, despite lifestyle modifications and pharmacological interventions using oral antidiabetic agents (OAD)^{7,8}. Therefore, at present, the initiation of insulin therapy is generally thought to be inevitable in a certain proportion of

T2D patients. However, how and when to initiate insulin therapy in T2D patients remains controversial.

In recent reports, once or twice daily use of basal insulin analogues as an add-on therapy to OAD (so-called basal-supported oral therapy [BOT]) in insulin-naïve T2D patients has shown that glargine or detemir can achieve clinically important improvements in glycaemic control, similar to those achievable with neutral protamine Hagedorn insulin, but with less risk of hypoglycaemia^{9–14}. On the basis of these results, the recent guidelines from Western countries have recommended that insulin should be initiated with basal insulin⁶. However, in a report of Japanese T2D patients, approximately half of the patients could not achieve a HbA_{1c} level of <7.0%¹⁵. In that study, no clear explanatory characteristics distinguished patients who could achieve good glycaemic control from those who did not.

In contrast to basal analogue insulin, premixed analogue insulin, such as biphasic insulin aspart 70/30 (BIAsp 30), can improve postprandial glucose levels and provide basal insulin

¹Department of Endocrinology, Diabetes and Geriatric Medicine, Akita University Graduate School of Medicine, Hondo, ²Akita Red Cross Hospital, Saruta, Kamikitate, ³Akita City Hospital, Kawamoto, ⁴Yokote Municipal Hospital, Yokote, ⁵Akita Kumiai General Hospital, Ijima, Akita, and ⁶Department of Medicine, Saitama Medical Center, Jichi Medical University, Omiya, Saitama, Japan
*Corresponding author. Takuma Narita Tel.: +81-18-884-6040 Fax: +81-18-884-6449
E-mail address: narita@med.akita-u.ac.jp
Received 13 January 2010; revised 18 June 2010; accepted 30 July 2010

coverage by one injection at mealtime. The ability of BIAsp 30 to improve postprandial glucose levels is superior to human premixed insulin 70/30^{16,17}. In the recent 'The 1-2-3 study', insulin therapy was initiated with once-daily pre-dinner BIAsp 30, titrated to a target fasting blood glucose (FBG) level of 80–110 mg/dL by add-on OAD therapies (phase 1), followed by the addition of pre-breakfast BIAsp 30 (phase 2) and pre-lunch BIAsp 30 (phase 3), with OAD withdrawal in patients showing a HbA_{1c} level $\geq 6.5\%$ at the end of phase 1 or 2. Just after phase 1, 2 and 3 of this regimen 41, 70 and 77%, respectively, of patients had a HbA_{1c} level of $< 7.0\%$ ¹⁸. A recent study that used a similar step-up regimen with BIAsp 30 in Japanese T2D patients¹⁹ confirmed the efficacy and usefulness of the method.

Quite recently, the regimen of adding a once-daily pre-dinner injection of BIAsp 30 has been reported to have equal or a slightly superior efficacy in improving glycemic control than those of basal insulin analogues as add-on OAD therapies²⁰. However, the efficacy and safety of this method in Japanese T2D patients has not yet been sufficiently tested. In particular, the differences in the clinical characteristics of patients who can or cannot achieve optimal glycemic control, including postprandial glycemic control, after this regimen need to be elucidated.

In an outpatient setting, patient-directed insulin dosage titration, according to a predetermined dosage-escalation algorithm, reportedly shows the same levels of improvement in glycemic control and safety as physician-led dosage titration^{21,22}.

We, therefore, investigated the extent to which a regimen with once-daily pre-dinner BIAsp 30 as an add-on OAD therapy would improve HbA_{1c} levels and daily profiles of blood glucose (BG) in Japanese T2D patients under OAD failure. In the present study, we used patient-directed insulin titration method on the basis of self-monitoring BG (SMBG) levels according to a predetermined algorithm. Furthermore, we attempted to identify differences in clinical characteristics between patients with and without optimal glycemic control after undergoing this regimen.

MATERIALS AND METHODS

Patients

Eligible patients were as follows: diagnosed with T2D for ≥ 1 year, ≥ 20 years-of-age, not pregnant, insulin naïve and HbA_{1c} levels of $> 7.0\%$ or fasting plasma glucose levels of ≥ 140 mg/dL on a standard regimen⁵ for ≥ 3 months with OAD. Sulfonylurea (SU) dosages were to be at least equivalent to a daily dose of 5 mg of glibenclamide, 80 mg of gliclazide or 3 mg of glimepiride with or without metformin (MET), thiazolidinedione (TZD) and/or alpha-glucosidase inhibitors (AGI). In addition, SMBG was introduced to eligible patients during the 4 weeks before initiation of BIAsp 30. Patients were instructed to monitor their FBG levels every day. Patients with FBG of ≥ 140 mg/dL (mean of the last 3 days during the 4-week SMBG period) were confirmed as final eligible patients. Enrolled patients did not have hepatic insufficiency (alanine transaminase or aspartate transaminase is ≥ 2 -fold of the upper reference limit of each institute), renal insufficiency (serum creatinine ≥ 1.4 mg/dL), severe diabetic complications

(overt proteinuria with renal failure, unstable proliferative retinopathy or symptomatic orthostatic hypotension), malignant tumors or dementia. We carried out this 24-week, open-label, interventional, multicenter (five hospitals in Akita Prefecture, Japan: Akita University Hospital, Akita Red Cross Hospital, Akita City Hospital, Akita Kumiai General Hospital and Yokote Municipal Hospital) study in accordance with the Declaration of Helsinki. All the patients provided written informed consent.

Medication and BIAsp 30 Titration

Eligible patients were instructed to add a once-daily BIAsp 30 injection within 15 min pre-dinner to their OAD regimens. Dosages of SU were reduced to the allowed minimum dosages for Japan (2.5 mg of glibenclamide, 40 mg of gliclazide or 1 mg of glimepiride) to avoid hypoglycemia, particularly during the night. MET, TZD and AGI were taken as baseline treatment in each patient. The initial dosage of BIAsp 30 was 3 U, followed by self-adjustment of the pre-dinner BIAsp 30 dosage every 3–4 days on the basis of an average of 3–4 previous FBG values. The dosage-titration algorithm was as follows:

Mean fasting SMBG (mg/dL)	≤ 80	81–100	101–120	121–140	141–160	160<
Adjustment of insulin dosage (U)	–3	–1	0	+1	+2	+3

On the basis of this method, the present study was named the 'STEP-AKITA study', abbreviated from SMBG based management of type 2 diabetes under oral antidiabetic drugs failure with evening premixed biphasic insulin aspart 70/30 injection in AKITA.

Patients were encouraged to visit an outpatient clinic every 2–4 weeks. If necessary, patients were allowed to consult their physicians about the adjustment of insulin dosages by phone or fax. BIAsp 30 was given with the prefilled (3 mL, 100 U/mL) Novorapid 30 mix FlexPen delivery system (Novo Nordisk, Bagsvaerd, Denmark).

Assessments

Blood samples for the assessment of HbA_{1c} levels were obtained every 4 weeks along with a routine examination of hepatic and renal function. HbA_{1c} levels and the proportion of patients achieving those of $< 7.0\%$ or $< 6.5\%$ at 16 and 24 weeks after the initiation of BIAsp 30 were assessed, as it is unclear how long an observation period needs to be for sufficient evaluation of the effect on HbA_{1c} levels in insulin therapies added to OAD. Patients were encouraged to record 8-point SMBG profiles (including pre- and post-breakfast, -lunch and -dinner profiles; bedtime and 03.00 h, where 'post' times were 2 h later) at least once a week. Because sufficient 8-point SMBG profiles were obtained in more patients around the time BIAsp 30 titration finished than at 16 or 24 weeks, 8-point SMBG profiles

recorded just before the initiation of BIAsp 30 (baseline) and just after BIAsp 30 titration was judged to be finished were used for evaluation. Bodyweight (BW) was recorded in the outpatient clinic once a month.

Patients were re-taught how to recognize the symptoms of hypoglycemia and were instructed to obtain and record their SMBG level whenever a hypoglycemic event was suspected. Hypoglycemic episodes were classified as mild when SMBG levels were <70 mg/dL, regardless of hypoglycemic symptoms, and when patients could manage themselves. Events were classified as severe when BG levels were <70 mg/dL and when patients were unable to manage themselves.

To detect any worsening of retinopathy, all patients were required to consult ophthalmologists before initiation of BIAsp 30 and after titration.

Laboratory Procedures

SMBG was carried out with provided BG (capillary) meters (One Touch Ultra, LifeScan, Milpitas, CA, USA). HbA_{1c} level was measured by high performance liquid chromatography using an automated analyzer at each hospital and values were calibrated with standard substances recommended by Japan Diabetes Society (JDS Lot 2). The reference range of HbA_{1c} levels is 4.3–5.8%. HbA_{1c} values were expressed as JDS values.

Statistical Analysis

Values are expressed as mean \pm SD. The Friedman test was used to identify global differences in values throughout the study period. Furthermore, values at each time after the initiation of BIAsp 30 were compared with the value at baseline using Dunn's multiple comparison test (non-parametric). The Wilcoxon signed-ranks test was used for paired comparisons between values before and after treatment. The Mann-Whitney *U*-test and Pearson's χ^2 -test were used to calculate the significance of differences in values between groups. Pearson's correlation analysis was carried out to explore relationships between corresponding values. All calculations were made using StatFlex Version 5.0 (Artec, Osaka, Japan). Two tailed *P*-values of <0.05 were considered statistically significant.

RESULTS

Participants

A total of 29 patients, with a mean fasting SMBG \geq 140 mg/dL, even in the last 3 days during the 4-week SMBG period, initiated BIAsp 30 according to the protocol. Of those, seven patients did not complete the study. Reasons for withdrawal were adverse events in two patients, (progression of diabetic retinopathy and skin allergy at injection site) and non-compliance of insulin injection or SMBG recording in five patients. Finally, 22 and 20 patients completed 16- and 24-week follow up of HbA_{1c} levels, respectively. The clinical characteristics of 22 patients are shown in Table 1. No patient had been treated with SU monotherapy. More than 80% of patients had been treated with MET or TZD.

Table 1 | Clinical characteristics of type 2 diabetic patients

Male/female (<i>n</i>)	10/12
Age (years)	62.1 \pm 5.0
Body mass index (kg/m ²)	25.1 \pm 5.0
Duration of diabetes (years)	13 \pm 9.4
Retinopathy (nil/simple/proliferative)	(15/7/0)
Albuminuria (normo/micro/macro)	(13/3/6)
HbA _{1c} at baseline (%)	8.5 \pm 1.5
No. OAD (%)	
Monotherapy	0 (0)
Combination therapy	
SU + MET	3 (13.6)
SU + TZD	3 (13.6)
SU + MET + TZD	11 (50.0)
SU + TZD + AGI	1 (4.5)
SU + MET + TZD + AGI	4 (18.2)
Use of MET	18 (81.8)
Use of TZD	19 (86.4)

Data are expressed as mean \pm SD or otherwise indicated.

AGI, alpha-glucosidase inhibitor; MET, metformin; OAD, oral anti-diabetic agents; SU, sulfonylurea; TZD, thiazolidinedione.

Glycemic Control

Efficacy Achieved as Per HbA_{1c} Levels

Achieved HbA_{1c} levels are shown in Figure 1a. At 8 weeks after the initiation of BIAsp 30, mean HbA_{1c} level was significantly decreased (7.4 \pm 1.2, *vs* 8.5 \pm 1.5% at baseline; *P* < 0.05). At 16 weeks, mean HbA_{1c} level had stabilized to 6.8 \pm 1.0% (*P* < 0.01 *vs* baseline) and showed a tendency toward a slight decrease until 24 weeks (at 24 weeks, 6.6 \pm 0.7%, *P* < 0.01 *vs* baseline). At 16 weeks, the rates of patients who achieved HbA_{1c} levels of <7.0 and <6.5% were 68.2% (15/22) and 45.5% (10/22), respectively. At 24 weeks, 16 of 20 (80.0%) and 7 of 20 (35.0%) patients had achieved HbA_{1c} levels of <7.0 and <6.5%, respectively. Reduction of the rate of patients achieving a HbA_{1c} level of <6.5% at 24 weeks was a result of worsening of HbA_{1c} level to \geq 6.5% in two patients and a patient dropping out before 24-week follow up, among 10 patients who achieved a HbA_{1c} level of <6.5% at 16 weeks. When the patients were stratified according to baseline HbA_{1c} levels of <8.0 or \geq 8.0%, 87.5% (7/8) and 75.0% (9/12) of patients, respectively, had achieved HbA_{1c} levels of <7.0% at 24 weeks. Further, 37.5% (3/8) and 33.3% (4/12) of patients with respective baseline HbA_{1c} levels of <8.0 and \geq 8.0% had achieved HbA_{1c} levels of <6.5% at 24 weeks. The rates of patients who had achieved HbA_{1c} levels of <7.0 and <6.5% as the final evaluations at 24 weeks were not influenced by baseline HbA_{1c} levels. Figure 2b shows a strong linear correlation between baseline HbA_{1c} levels and change in HbA_{1c} levels from the baseline (Δ HbA_{1c}) at 24 weeks in 20 patients (Figure 2b), showing that an even higher HbA_{1c} level at baseline can be lowered sufficiently by the regimen of the present study.

Efficacy Achieved as Per Daily Profiles of SMBG

Figure 1b shows the improvement in 8-point SMBG profiles in 21 patients whose daily 8-point SMBG profiles at baseline and

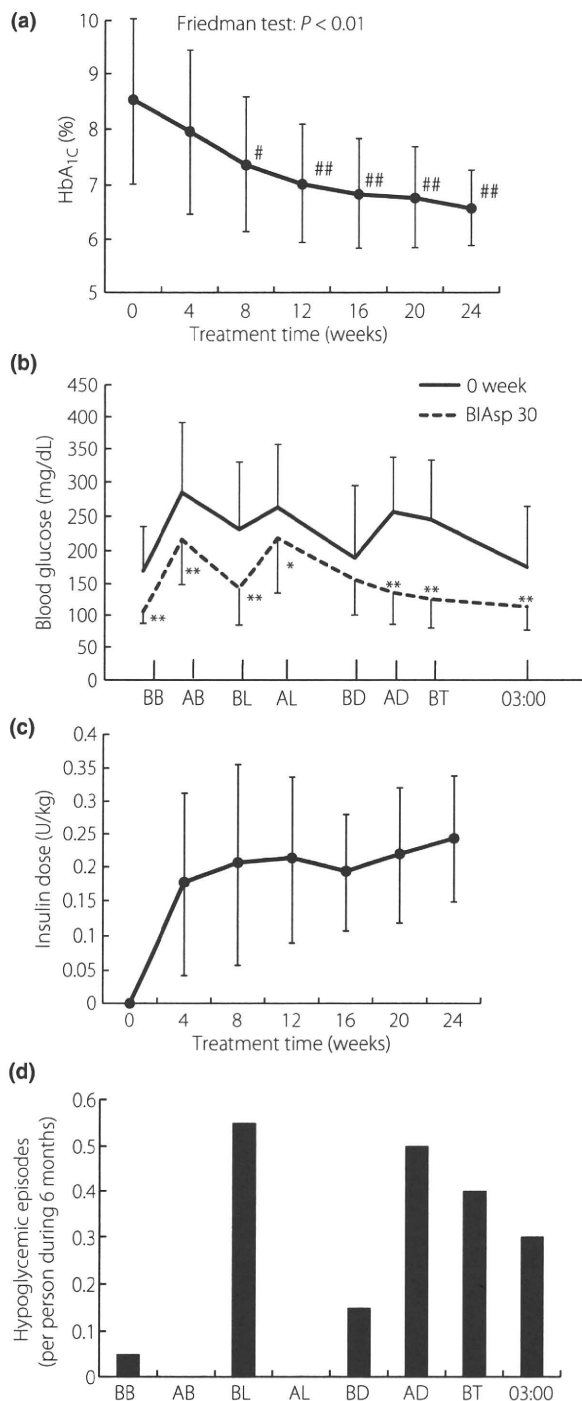


Figure 1 | Clinical parameters during the treatment with pre-dinner biphasic insulin aspart 70/30. (a) Changes in HbA_{1c}. (b) Mean 8-point self-monitored blood glucose profiles at baseline and just after BIAsp 30 titration. (c) Changes in self-titrated insulin dose. (d) Incidences of hypoglycemic episodes. Data are expressed as mean ± SD in a, b and c. AB, 2 h post-breakfast; AD, 2 h post-dinner; AL, 2 h post-lunch; BB, pre-breakfast; BD, pre-dinner; BL, pre-lunch; BT, bed time. #*P* < 0.05; ##*P* < 0.01 versus values at 0 week revealed by Dunn's multiple comparison test. **P* < 0.05; ***P* < 0.01 versus values at 0 week revealed by the Wilcoxon signed-ranks test.

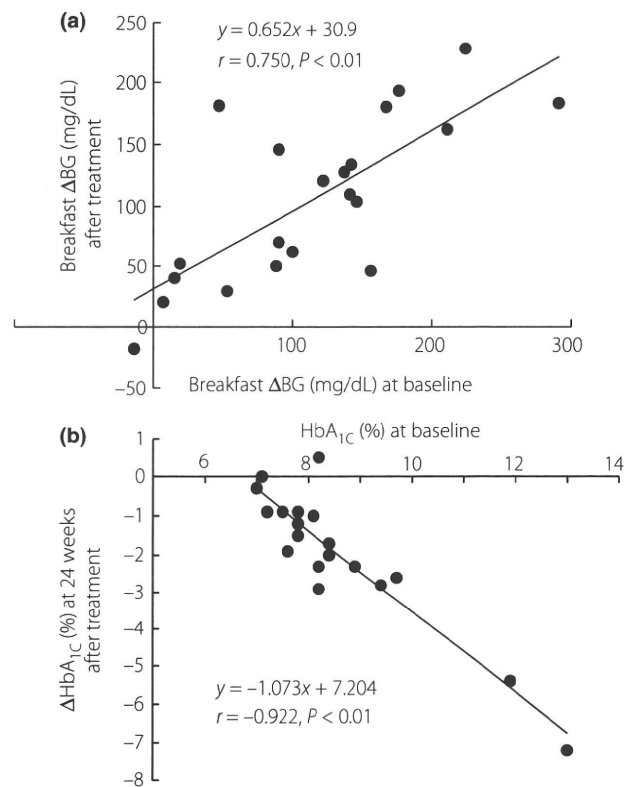


Figure 2 | Relationships (a) between post-breakfast blood glucose excursion (ΔBG) at baseline and that just after titration of pre-dinner biphasic insulin aspart 70/30 and (b) between baseline HbA_{1c} levels (%) and changes in HbA_{1c} levels (ΔHbA_{1c}, %) at 24 weeks from baseline.

just after BIAsp 30 titration (after titration) were sufficiently obtained. All the points of BG measured were significantly decreased, except for pre-dinner BG. In particular, the decreases in BG at pre- and post-breakfast, pre-lunch, post-dinner, at bedtime and at 03.00 h were remarkable (*P* < 0.01). As shown in Figure 1b, the BG profiles from post-dinner to pre-breakfast were well stabilized without post-dinner BG excursion (ΔBG) after titration (67.1 ± 85.4 mg/dL at baseline and -23.6 ± 67.4 mg/dL after titration; *P* < 0.01), whereas post-breakfast ΔBG after BIAsp 30 titration remained comparable to that at baseline (114.7 ± 77.9 mg/dL at baseline and 105.8 ± 67.7 mg/dL after titration).

Clinical Characteristics of Patients With or Without Optimal Post-breakfast ΔBG Pattern After Treatment

The patients in the present study showed widely divergent post-breakfast ΔBG (from -18 to 228 mg/dL) even after nearly ideal FBG levels had been established by BIAsp 30 titration (Fig. 2a). Therefore, clinical characteristics with or without optimal post-breakfast ΔBG after titration were explored. Individual post-breakfast ΔBG at baseline and after BIAsp 30 titration showed a strong correlation (Fig. 2a), indicating that the treatment might scarcely influence the individual post-breakfast ΔBG pattern. Therefore, we divided the patients into two groups according to

Table 2 | Clinical characteristics of type 2 diabetic patients divided according to 2-h post-breakfast blood glucose levels after biphasic insulin aspart 70/30 titration

	Blood glucose at 2 h after breakfast		
	<200 mg/dL <i>n</i> = 10 (Group A)	≥200 mg/dL <i>n</i> = 11 (Group B)	<i>P</i> -value
Male/female (<i>n</i>)	8/2	4/7	<0.05
Age (years)	55.3 ± 5.7	66.8 ± 10.5	<0.05
Body mass index (kg/m ²)	25.3 ± 4.1	24.6 ± 6.4	NS
Duration of diabetes (years)	8.7 ± 7.0	18.9 ± 11.7	<0.05
AGI use (<i>n</i> , %)	3, 30.0	2, 18.1	NS
HbA _{1c} levels at 0 week (%)	8.9 ± 1.8	8.7 ± 2.0	NS
HbA _{1c} levels at 16 weeks (%)	6.7 ± 0.62	6.8 ± 0.96	NS
ΔHbA _{1c} 0–16 weeks (%)	−2.2 ± 1.9	−1.9 ± 1.4	NS
FBG at 0 week (mg/dL)	173.8 ± 80.0	166.3 ± 52.8	NS
2h-BG-M at 0 week (mg/dL)	239.3 ± 119.3	325.6 ± 71.6	NS
ΔBG-M at 0 week (mg/dL)	65.5 ± 58.5	159.4 ± 66.6	<0.01
FBG after BIAsp 30 titration (mg/dL)	106.7 ± 14.5	109.9 ± 19.8	NS
2h-BG-M after BIAsp 30 titration (mg/dL)	152.8 ± 29.5	269.9 ± 36.9	<0.01
ΔBG-M after BIAsp 30 titration (mg/dL)	46.2 ± 33.5	160.0 ± 36.9	<0.01
Insulin dosage after BIAsp 30 titration (U/kg)	0.21 ± 0.14	0.23 ± 0.15	NS

Data are expressed as mean ± SD or otherwise indicated. The Mann–Whitney *U*-test and Pearson's χ^2 -test was used to calculate statistically significant differences of the values between groups. 2h-BG-M, blood glucose 2 h after breakfast; ΔHbA_{1c} 0–16 weeks, changes in HbA_{1c} levels from baseline to 16 weeks; AGI, alpha-glucosidase inhibitor; FBG, fasting blood glucose; ΔBG-M, blood glucose excursion for 2 h after breakfast; NS, not significant.

post-breakfast SMBG levels after BIAsp 30 titration: Group A, <200 mg/dL; and Group B, ≥200 mg/dL (Table 2). Figure 3 shows the daily 8-point SMBG profiles at baseline and after BIAsp 30 titration, indicating relatively flat BG profiles in Group A and ruggedness in Group B. Table 2 shows the clinical characteristics of both groups. Patients in Group B had a greater proportion of women, older age, longer duration of diabetes and higher post-breakfast ΔBG both before and after BIAsp 30 titration. Despite the rugged daytime BG profiles, even after BIAsp 30 titration, HbA_{1c} levels after BIAsp 30 treatment in Group B were not significantly higher compared with that in Group A (Table 2).

Insulin Dosages

Insulin dosage (U/kg) was titrated to 0.18 ± 0.14 at 4 weeks, 0.19 ± 0.09 at 16 weeks, 0.22 ± 0.10 at 20 weeks and 0.24 ± 0.09 at 24 weeks (Figure 1c).

BW Changes

BW changes from 0 week (kg) were −0.12 ± 1.0, 0.23 ± 1.8, 0.59 ± 2.3, 1.1 ± 2.2, 1.9 ± 2.8 and 2.5 ± 2.7 at 4, 8, 12, 16, 20

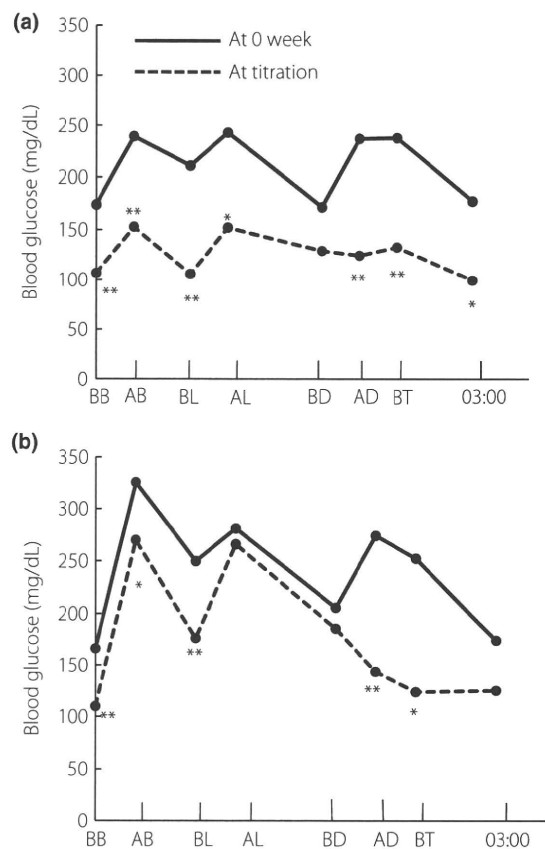


Figure 3 | Mean 8-point self-monitored blood glucose (BG) profiles at 0 week and just after pre-dinner biphasic insulin aspart 70/30 (BIAsp 30) titration (a) in patients with 2 h post-breakfast BG after BIAsp 30 titration <200 mg/dL and (b) in patients with 2 h post-breakfast BG after BIAsp 30 titration ≥200 mg/dL. AB, 2 hours post-breakfast; AD, 2 h post-dinner; AL, 2 h post-lunch; BB, pre-breakfast; BD, pre-dinner; BL, pre-lunch; BT, bed time. **P* < 0.05; ***P* < 0.01 versus values at 0 week revealed by the Wilcoxon signed-ranks test.

and 24 weeks, respectively. The Friedman test showed significant BW changes throughout the study period (*P* < 0.01). BW at 20 and 24 weeks were significantly increased compared with baseline (*P* < 0.05 by Dunn's multiple comparison test).

Hypoglycemic Episodes and Adverse Events

No severe hypoglycemic episodes were reported. Mild hypoglycemic episodes were reported by 13 of 29 patients (including 7 patients who withdrew from the study) during the study at a low rate of 1.95 events per patient over the course of 6 months (Figure 1d). Principally, patients had experienced hypoglycemic episodes pre-lunch, post-dinner, at bedtime and at 03.00 h.

One woman withdrew because of a progression of diabetic retinopathy (progression from no clinical lesions at baseline to proliferative retinopathy requiring photocoagulation and surgical procedure by an ophthalmologist 6 weeks after initiation of

BIAsp 30). Another woman withdrew because of skin allergy at the injection site. The patient with a marked retinopathy progression mentioned previously had a long estimated duration of diabetes (23 years) and marked poor glycemic control (HbA_{1c} level at baseline of 13.8%, Δ HbA_{1c} at 4, 8 and 12 weeks of -2.7 , -3.8 and -4.5% , respectively). Retinopathy progression was reported in another two patients who were able to complete the study. In one woman, simple retinopathy before the initiation of BIAsp 30 had progressed to proliferative retinopathy 1 month after the end of this study (HbA_{1c} levels at baseline and at 24 weeks were 7.8, 6.9%, respectively. Δ HbA_{1c} at 4, 8 and 12 weeks were -0.5 , -0.6 and -0.7% , respectively). In another patient, a man without retinopathy at baseline, simple retinopathy was found 24 months after the end of the present study (HbA_{1c} levels at baseline and at 24 weeks were 7.2 and 6.3%, respectively. Δ HbA_{1c} at 4, 8 and 12 weeks were -0.3 , -1.1 and -1.6% , respectively).

DISCUSSION

This study showed that in Japanese T2D patients with failed OAD therapies, patients who had achieved optimal glycemic control, including daytime postprandial BG profiles after an addition of appropriate dosage of once-daily pre-dinner BIAsp 30 (Group A), had lower post-breakfast BG excursions at baseline, shorter diabetes durations and younger age. The other patients with opposite clinical characteristics (Group B) had still shown higher daytime postprandial BG excursions, even after achievement of ideal BG profiles from post-dinner to pre-breakfast, by the regimen used in the present study.

In Group A patients, the ranges of daily BG profiles before and after BIAsp 30 titration were relatively flat (Figure 3) and resembled those of T2D patients from Western countries, who used BOT or pre-dinner BIAsp 30 as an add-on to OAD^{9-14,18,20}. Additionally, daily BG profiles after titration were ideal and didn't seem to require additional insulin supplementation at breakfast or lunch. In contrast, Group B patients had higher daytime postprandial glucose excursions both before and after BIAsp 30 titration and higher baseline post-breakfast Δ BG levels were preserved even after treatment (Figure 3), requiring bolus dosages at breakfast and/or lunch time to achieve ideal daily BG profiles. Collectively, higher post-breakfast Δ BG levels with OAD failure might predict a need for two or more bolus supplements of insulin after the establishment of ideal BG profiles from post-dinner to pre-breakfast by pre-dinner BIAsp 30 titration.

Group B patients had relatively higher age and longer durations of diabetes (Table 2), indicating that they had the characteristics of more declined β -cell function reported in long-standing T2D patients^{7,8}. The main characteristics of Asian T2D patients have been thought to include declined β -cell function²³⁻²⁵ and a loss of early-phase insulin response²⁶. Taking these findings together, Japanese T2D patients with OAD failure can be divided into two groups: one characterized with relatively declined β -cell function with higher postprandial glucose

excursions requiring appropriate basal and multiple bolus insulin supplements; and the other with relatively preserved β -cell function with lower postprandial glucose excursions requiring only appropriate FBG correction that might be achieved with the addition of once-daily injections to OAD therapies, such as pre-dinner BIAsp 30 or basal insulin analogues.

Table 2 shows that there is no difference in HbA_{1c} levels at 16 weeks between Group A and B, despite the markedly different patterns of daytime BG excursion (Figure 3). It is difficult to explain this phenomenon. Daily SMBG profiles had been well preserved during the study (the post-breakfast Δ BG last recorded during the study in Group A and B were 57.6 ± 55.5 and 141.7 ± 55.5 mg/dL [$P < 0.01$], respectively). Postprandial glucose spikes of relatively short duration might have minor effects on HbA_{1c} levels. Because glycated albumin (GA) is reported to be a more sensitive marker than HbA_{1c} for glucose excursions²⁷, we would have measured GA levels in the present study.

The results that 80 and 35% of participants were able to achieve HbA_{1c} levels of <7.0 and $<6.5\%$, respectively, at 24 weeks confirmed the satisfactory results of phase 1 in 'The 1-2-3 study' (in which HbA_{1c} level was $<7.0\%$ in 41% and $<6.5\%$ in 21% of patients)¹⁸. Recently, it was reported that HbA_{1c} levels of 7.0 and 6.5% in the USA are equivalent to those of 6.6 and 6.1% in Japan (JDS values)²⁸. Considering the methodological differences used to determine HbA_{1c} levels between Japan and the USA, the result that 35% of the patients in the present study achieved HbA_{1c} levels of $<6.5\%$ (equivalent to 6.9% in the USA) is comparable to the result of 'The 1-2-3 study'. Recent guidelines from Western countries recommend that insulin should be initiated with basal insulin analogues as add-on OAD therapies⁶. However, the satisfactory results of 'The 1-2-3 study', the study of Strojek *et al.*²⁰ and the present study show that adding a once-daily pre-dinner injection of BIAsp 30 in T2D patients with OAD failure might represent an alternative regimen at the initiation of insulin therapy.

The present study used an insulin titration method managed by patients themselves on the basis of SMBG levels according to a predetermined algorithm^{21,22}. The satisfactory effects of the present study on HbA_{1c} levels with a minimal incidence of hypoglycemia also confirmed the usefulness of this insulin titration method in Japanese T2D patients. Dosage-adjustment levels at each correction were designed to be approximately one-third of those applied in Western countries^{18,21,22}, where the body mass index (BMI) of patients is approximately 30. The BMI of our patients was approximately 25, suggesting a less insulin-resistant feature of Japanese T2D patients and the need for a finer insulin titration regimen.

In the present study, no severe hypoglycemic episodes were recorded and the frequency of mild hypoglycemic episodes was considered acceptable. Recording SMBG, especially pre-breakfast everyday and self-adjustment of pre-dinner BIAsp 30 dosage, according to SMBG levels might be related to this level of safety. The reduced dosages of SU at the initiation of BIAsp 30 in the